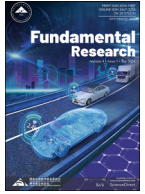


Contents lists available at ScienceDirect

## Fundamental Research

journal homepage: <http://www.keaipublishing.com/en/journals/fundamental-research/>

## Review

## On networks of space-based gravitational-wave detectors

Rong-Gen Cai<sup>a,b,c,1,\*</sup>, Zong-Kuan Guo<sup>a,c,d,1,\*</sup>, Bin Hu<sup>e,1,\*</sup>, Chang Liu<sup>c,d,f,1,\*</sup>, Youjun Lu<sup>g,h,1,\*</sup>, Wei-Tou Ni<sup>i,j,1,\*</sup>, Wen-Hong Ruan<sup>c,d,1,\*</sup>, Naoki Seto<sup>k,1,\*</sup>, Gang Wang<sup>l,1,\*</sup>, Yue-Liang Wu<sup>a,c,m,1,\*</sup>

<sup>a</sup> CAS Key Laboratory of Theoretical Physics, Institute of Theoretical Physics, Chinese Academy of Sciences, Beijing 100190, China<sup>b</sup> School of Physical Science and Technology, Ningbo University, Ningbo 315211, China<sup>c</sup> School of Fundamental Physics and Mathematical Sciences, Hangzhou Institute for Advanced Study, University of Chinese Academy of Sciences, Hangzhou 310024, China<sup>d</sup> School of Physical Sciences, University of Chinese Academy of Sciences, Beijing 100049, China<sup>e</sup> Department of Astronomy, Beijing Normal University, Beijing 100875, China<sup>f</sup> Center for Gravitation and Cosmology, College of Physical Science and Technology, Yangzhou University, Yangzhou, 225009, China<sup>g</sup> National Astronomical Observatories, Chinese Academy of Sciences, Beijing, 100101, China<sup>h</sup> School of Astronomy and Space Science, University of Chinese Academy of Sciences, Beijing, 100049, China<sup>i</sup> International Centre for Theoretical Physics Asia-Pacific, University of Chinese Academy of Sciences, Beijing 100049, China<sup>j</sup> State Key Laboratory of Magnetic Resonance and Atomic and Molecular Physics, Innovation Academy for Precision Measurement Science and Technology (APM), Chinese Academy of Sciences, Wuhan 430071, China<sup>k</sup> Department of Physics, Kyoto University, Kyoto 606–8502, Japan<sup>l</sup> Shanghai Astronomical Observatory, Chinese Academy of Sciences, Shanghai, 200030, China<sup>m</sup> International Centre for Theoretical Physics Asia-Pacific, Beijing/Hangzhou, China

## ARTICLE INFO

## Article history:

Received 31 May 2023

Received in revised form 1 August 2023

Accepted 10 October 2023

Available online 8 November 2023

## Keywords:

Gravitational waves

Detector networks

LISA

Taiji

Tianqin

Massive binary black holes

Galactic binaries

Stochastic gravitational wave background

## ABSTRACT

The space-based laser interferometers, LISA, Taiji and TianQin, are targeting to observe milliHz gravitational waves (GWs) in the 2030s. The joint observations from multiple space-based detectors yield significant advantages. In this work, we recap the studies and investigations for the joint space-based GW detector networks to highlight: 1) the high precision of sky localization for the massive binary black hole (BBH) coalescences and the GW sirens in the cosmological implication, 2) the effectiveness to test the parity violation in the stochastic GW background observations, 3) the efficiency of subtracting galactic foreground, 4) the improvement in stellar-mass BBH observations. We inspect alternative networks by trading off massive BBH observations and stochastic GW background observation.

## 1. Introduction

The sky localization of gravitational-wave (GW) sources is one of key scientific tasks for GW observations. Rapid and accurate localization is crucial to help follow-up observations of their electromagnetic counterparts. Once their host galaxies are uniquely identified by observations of their electromagnetic counterparts, these GW events can be used as standard sirens to measure the cosmological parameters [1]. If GW events

are not accompanied by electromagnetic counterparts, these GW events, as so-called dark sirens, can measure the cosmological parameters by statistical techniques using galaxy catalogues. In this case, precision localization of GW sources reduces the number of possible host galaxies, which improves measurements of the cosmological parameters. However, a single laser interferometer detector is insensitive to the sky location of transient GW sources. In principle, the location of sources can be determined by triangulation based on the differences in times of arrival

\* Corresponding authors.

E-mail addresses: [cairg@itp.ac.cn](mailto:cairg@itp.ac.cn) (R.-G. Cai), [guozk@itp.ac.cn](mailto:guozk@itp.ac.cn) (Z.-K. Guo), [bhu@bnu.edu.cn](mailto:bhu@bnu.edu.cn) (B. Hu), [liuchang@alumni.itp.ac.cn](mailto:liuchang@alumni.itp.ac.cn) (C. Liu), [luyj@nao.cas.cn](mailto:luyj@nao.cas.cn) (Y. Lu), [weitou@gmail.com](mailto:weitou@gmail.com) (W.-T. Ni), [ruanwenhong@ucas.ac.cn](mailto:ruanwenhong@ucas.ac.cn) (W.-H. Ruan), [seto@tap.scphys.kyoto-u.ac.jp](mailto:seto@tap.scphys.kyoto-u.ac.jp) (N. Seto), [gwang@shao.ac.cn](mailto:gwang@shao.ac.cn) (G. Wang), [ylwu@ucas.ac.cn](mailto:ylwu@ucas.ac.cn) (Y.-L. Wu).

<sup>1</sup> All authors are ordered by their names.

at the different detector sits in a network of more than three detectors. Actually, including the amplitude and phase of the signal enables the source to be localized to a single sky path in a network of three detectors.

The two detectors of advanced LIGO in the United States, one in Hanford, Washington and the other in Livingston, Louisiana, simultaneously observed the first GW signal from the coalescence of stellar-mass binary black hole (BBH), GW150914 [2]. During the second observing run, the advanced Virgo detector near Pisa, Italy, joined the two advanced LIGO detectors. The GW event of GW170814 was for the first time observed with a network of three detectors [3]. Such a network improves the sky localization of the source, reducing the 90% credible area on the sky from 1160 deg<sup>2</sup> using only two advanced LIGO detectors to 60 deg<sup>2</sup> with the LIGO-Virgo network. For the signal of GW170817 from a binary neutron star inspiral, the source was localized to a region of 190 deg<sup>2</sup> using only two advanced LIGO detectors [4]. Although the signal is not visible in the Virgo data, adding the Virgo data allowed a precise sky localization to an area of 28 deg<sup>2</sup>. This measurement played an important role in identifying the host galaxy, NGC 4993. The KAGRA detector located in Japan will join the LIGO-Virgo network during the fourth observing run. The LIGO-Virgo-KAGRA network of four detectors are expected to improve the sky localization of GW sources. LIGO-India is a planned GW detector that will be located in India as part of the global network. Adding the LIGO-India detector to the existing LIGO-Virgo-KAGRA network will further improve the localization accuracy.

Unlike ground-based GW observations, a single space-based GW detector is able to localize the sky position of GW sources including massive BBHs, galactic binaries (GBs) in the Milk Way and extreme mass ratio inspirals. Such sources are usually visible to the detector for several days, months, or even years. Since the detector is moving relative to sources, the detector can be effectively regarded as a network of multiple detectors in different locations at different times. However, a single space-based GW detector could not accurately determine the source position on the sky. For example, LISA, a space observatory project proposed by the European Space Agency, achieves an angular resolution of about 0.3 square degrees for the coalescence of massive black hole binaries [5]. LISA is planned to launch between 2030 and 2035 [6]. Taiji proposed by the Chinese Academy of Sciences is expected to launch during the same period as LISA. If Taiji joins LISA, the LISA-Taiji network is expected to significantly improve the sky localization of massive BBHs [7]. For a BBH with a total mass of 10<sup>5</sup> solar mass, the LISA-Taiji network may improve the source localization by four orders of magnitude compared to an individual detector [8]. This result implies that it is possible to completely identify the host galaxy only from GW observations prior to the merger.

Besides improving the localization accuracy, the network of detectors increases the detection rate and improves the isotropy of the network antenna pattern [9]. Seto pointed out that the network is able to measure the Stokes parameter of GWs, which characterizes the asymmetry of the amplitudes of right- and left-handed waves [10]. Such the asymmetry is closely related to parity violation in the early Universe. This paper presents some significant progresses on the study for the space-based GW detector networks. We shall focus on the sky localization of sources, test of parity violation, subtraction of the galactic foreground, and improvement of the detection number of stellar BBHs.

The organization of this paper is as follows. In Section 2 we introduce the conception of space-based GW detector networks. We show that the localization accuracy of massive black hole binaries can be significantly improved by the LISA-Taiji network. This facilitates the cosmological implications such as standard sirens and dark sirens. In Section 3 we illustrate the effectiveness to test the parity violation in the stochastic GW background (SGWB). Section 4 presents the galactic foreground subtraction with space-based GW detector networks. In Section 5 we present the improvement of the detection number of stellar BBHs by the LISA-Taiji

network. In Section 6 alternative networks are discussed. Section 7 is our conclusions and prospects.

## 2. Localization of sources

In GW observations, the ability to quickly and accurately locate GW sources is crucial for advancing our understanding of the universe. Currently, the second-generation ground-based laser interferometer GW detectors, such as advanced LIGO and Virgo, are designed to primarily detect transient GW signals emitted from coalescing stellar-mass compact binaries. The detectors are most sensitive in the frequency band of 10–1000 Hz. The sensitivity of the detectors to GWs is not directional, which makes it challenging to precisely localize the sky position of a GW source using a single detector. However, with a network of three or more detectors, the sky position can be inferred by triangulation and analyzing the differences in the phase and amplitude detected by each detector. Unlike ground-based detectors, the space-based GW detectors focus on GW signals within frequency range of 10<sup>−4</sup> – 10<sup>−1</sup> Hz, which covers many types of sources [6,11–13]. In general, the GW signals can be observed by a space-based detector for extended periods of time, ranging from several days to years. As the detector moves and rotates in space, its sensitivity to different directions in the sky described by antenna pattern function changes, which allows for a precise determination of the source position.

### 2.1. Localization accuracy of coalescing massive BBHs

Particularly, the coalescing massive BBHs with total masses between 10<sup>4</sup> M<sub>⊙</sub> and 10<sup>8</sup> M<sub>⊙</sub> which emit GW signals accumulating large signal-to-noise ratios (SNRs) in a matter of days or weeks are primary sources of space-based GW detection [6,12,14]. The systems may also produce electromagnetic emission that can be detected by electromagnetic observations [15]. The fast and accurate localization of these sources from GW observations is significant for uniquely identifying the host galaxy, and it allows the detailed arrangements for follow-up electromagnetic spectroscopic observations. For a detected GW signal with a significant SNR, the uncertainties in the measurement of source parameters can be estimated by Fisher information matrix, and the elements of the matrix is given by [16]

$$\Gamma_{ij} = \sum_{\text{det}} \left( \frac{\partial h}{\partial \lambda_i} \middle| \frac{\partial h}{\partial \lambda_j} \right)_{\text{det}}, \quad (1)$$

where  $h$  is the GW waveform in frequency domain and  $\lambda_i$  denotes the  $i$ -th source parameter. In Eq. 1, the summation is operated on multiple detectors and the noise-weighted inner product  $\langle g|h \rangle$  is given by

$$\langle g|h \rangle = 4\Re \int_0^\infty \frac{g^*(f)h(f)}{S(f)} df, \quad (2)$$

where  $S(f)$  is the one-sided power spectral density of the detector noise. Considering the leading order, the variance-covariance matrix of the source parameters can be obtained by [16]

$$\sigma_{ij} = \langle \Delta \lambda_i \Delta \lambda_j \rangle = (\Gamma^{-1})_{ij}. \quad (3)$$

We can deduce the sky position of a GW source from the parameters: luminosity distance  $d_L$  and sky coordinates  $(\theta, \phi)$ . The uncertainty of the sky coordinates can be converted into the angular resolution  $\Delta\Omega_S$  by [8]

$$\Delta\Omega_S = 2\pi |\sin\theta| \sqrt{\langle \Delta\theta^2 \rangle \langle \Delta\phi^2 \rangle - \langle \Delta\theta\Delta\phi \rangle^2}, \quad (4)$$

where  $\langle \Delta\theta^2 \rangle$ ,  $\langle \Delta\phi^2 \rangle$  and  $\langle \Delta\theta\Delta\phi \rangle$  are given in Eq. 3. The luminosity distance uncertainty  $\Delta d_L/d_L$  can also be directly derived by Eq. 3.

Many studies have analyzed the localization accuracy of coalescing massive BBHs for LISA, Taiji or TianQin using the Fisher information matrix approach [8,16–25]. Their results indicate that it is not enough for a single space-based GW detector to uniquely identify the host galaxy

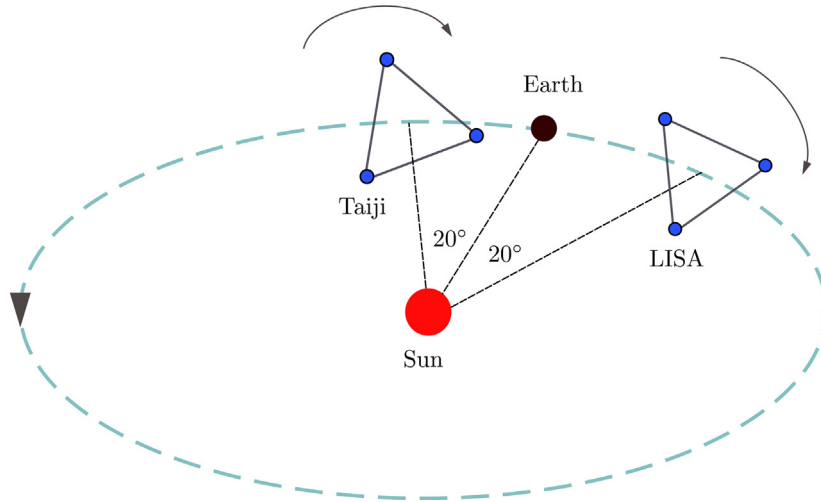


**Fig. 1.** Configuration of the LISA-Taiji network. The LISA constellation follows the Earth by  $20^\circ$ , while the Taiji constellation leads the Earth by  $20^\circ$ .

of a non-precession massive BBH from inspiral GW observations. However, considering that LISA, Taiji and TianQin would launch in the same period, it is feasible to conduct joint GW observations with multiple detectors. The performance of the multi-detector network on sky localization can also be estimated by above equations. The results in Ref [18] indicate that the localization accuracy of massive BBHs can be dramatically improved by a network of two or three LISA-like detectors. Specifically, some authors present the demonstration of the LISA-Taiji network in Ref [7]. For the network, the configuration angle subtended by the heliocentric orbit between LISA and Taiji is set at  $40^\circ$  (see Fig. 1). The LISA constellation follows the Earth by  $20^\circ$ , while the Taiji constellation leads the Earth by  $20^\circ$ . In fact, for the LISATaiji network, the configuration angle will affect the angular resolution of massive BBHs. According to the analysis of 10,000 equal-mass BBHs distributed at different sky positions with total intrinsic mass  $M = 10^5 M_\odot$  and redshift  $z = 1, 3$ , the minimum value of the angular resolution  $\Delta\Omega_s$  will be reached at a configuration angle of  $180^\circ$  [7]. As the configuration angle increases from  $3^\circ$  to  $40^\circ$ , there is an approximate improvement of 2 orders of magnitude in the median value of  $\Delta\Omega_s$ . Nevertheless, the improvement reduces to approximately 0.6 orders of magnitude as the configuration angle further increases from  $40^\circ$  to  $180^\circ$ . Thus, considering the potential cost of placing LISA or Taiji in space, it is reasonable to set the configuration angle at  $40^\circ$  for accurately localizing the GW sources. Moreover, other alternative network configurations have also been contemplated by some authors [25,26], and more details will be provided in Section 6.

The network of multiple space-based detectors provide a prospect to identify the host galaxy of massive BBHs before the final merger. For a given GW signal observed 52 days prior to merger, Taiji can localize the massive BBH with  $\Delta\Omega_s < 4 \text{ deg}^2$  and  $\Delta d_L/d_L < 8\%$  through the observation of the inspiral phase, while the LISA-Taiji network can localize the massive BBH with  $\Delta\Omega_s < 0.005 \text{ deg}^2$  and  $\Delta d_L/d_L < 0.5\%$  (see Fig. 2) [8]. In this case, the GW source is an equal-mass BBH with total intrinsic mass  $M = 10^5 M_\odot$  and redshift  $z = 1$ . The LISA-Taiji network has the ability to narrow the source localization region by about four orders of magnitude in comparison to a single detector, and the conclusion remains valid for the scenarios of  $M = 10^6 M_\odot$  and  $M = 10^7 M_\odot$  [8]. For massive BBHs with different inclination angles and sky positions, the LISA-Taiji network can still provide great improvement on the localization accuracy. Fig. 3 shows the variation of the angular resolution  $\Delta\Omega_s$  (left panel) and the luminosity distance uncertainty  $\Delta d_L/d_L$  (right panel) with redshift for Taiji and the LISA-Taiji network. For a fixed redshift in the figure, the median value and the  $1\sigma$  uncertainty range are calculated from 10,000 simulated equal-mass BBHs with fixed total intrinsic mass  $M = 10^5 M_\odot$  but random inclination angles and sky direc-

tions. Assuming a uniform distribution of galaxies in comoving volume with a number density of  $0.02 \text{ Mpc}^{-3}$ , the LISA-Taiji network has the capability to identify the host galaxy of the massive BBH with a total intrinsic mass of  $M = 10^5 M_\odot$  when satisfying the redshift  $z < 0.75$  [8]. It is estimated that the host galaxies of massive BBHs with  $M = 10^6 M_\odot$  and  $M = 10^7 M_\odot$  can be identified for  $z < 0.96$  and  $z < 0.45$ , respectively. Furthermore, for unequal-mass BBHs with component masses  $(10^7, 3.3 \times 10^6) M_\odot$ ,  $(10^6, 3.3 \times 10^5) M_\odot$  and  $(10^5, 3.3 \times 10^4) M_\odot$ , the LISA-Taiji network can improve the angular resolution by more than one order of magnitude compared to individual LISA or Taiji [23]. In addition to the LISA-Taiji network, the LISA-TianQin network can also bring comparable improvement on localization accuracy of massive BBHs, and it will be further improved by several times with the network of all three detectors [24,25,27].

Although the Fisher information matrix approach is convenient for statistical analysis of parameter uncertainties, it is only effective for a GW signal with large SNR. For a single detector, the approach cannot always provide reliable estimations of parameter uncertainties [25]. Therefore, some authors produce the posterior of parameters through the Bayesian inference to compare the localization accuracy of a single detector and a network of detectors [25,28]. The posterior samples of parameters can be given by many sampling method, such as Markov-chain Monte Carlo method [29] and Nested sampling method [30]. For more massive MBHBs, the results in Ref [25] indicate that the network of multiple detectors can improve the angular resolution by up to a few orders of magnitude and the luminosity distance uncertainty by up to 1 order of magnitude, which is consistent with the conclusion inferred by Fisher information matrix. Moreover, according to the Bayesian analysis for MBHBs with masses at orders of  $10^6 M_\odot$  and ecliptic latitude at  $\{30^\circ, 60^\circ, 90^\circ\}$ , a network of detectors is capable of improving the angular resolution by 1 order of magnitude [28]. In the special case of  $60^\circ$ , the improvement can even reach 4 orders of magnitude.

## 2.2. Localization accuracy of galactic binaries

Numerous compact binaries in the Milky Way are also potential sources of space-based GW detectors [6,12,14]. The components of these GBs can be neutron stars, white dwarfs and stellar-mass black holes. The GBs emit continuous and nearly monochromatic GW signals which are highly overlapped in the sensitive band of space-based GW detectors. Although most of the signals form an unresolved foreground for the detectors, it is expected that tens of thousands will be individually resolved with source parameters [31–33]. Moreover, electromagnetic observations have confirmed the existence of some GBs known as “verification binaries”, which provides guaranteed sources for joint gravi-

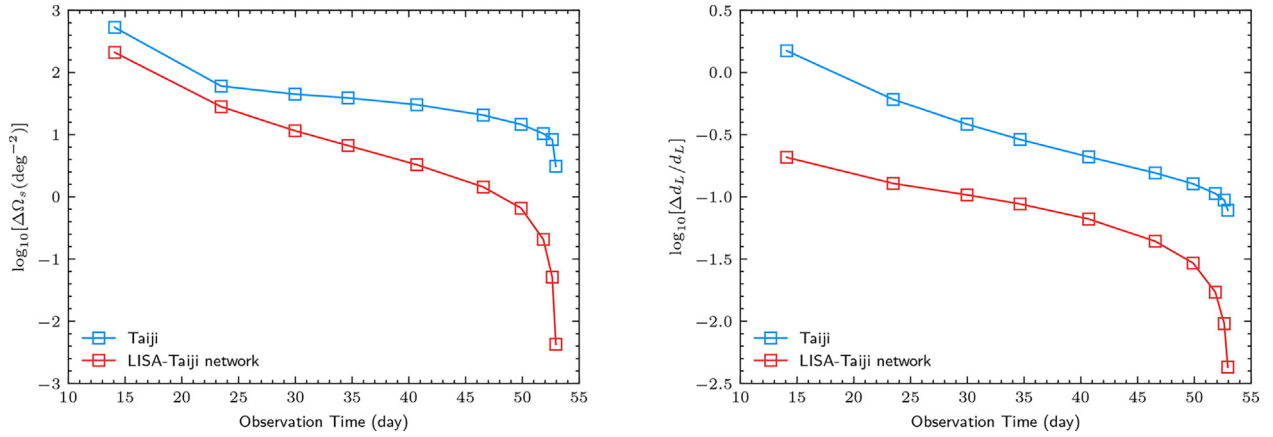


**Fig. 2.** The variation of the angular resolution  $\Delta\Omega_s$  (left panel) and the luminosity distance uncertainty  $\Delta d_L/d_L$  (right panel) with observation time for Taiji (blue) and the LISA-Taiji network (red). The GW source is chosen to an equal-mass BBH with total intrinsic mass  $M = 10^5 M_\odot$  and redshift  $z = 1$ . Figures from Ref [8]. (For interpretation of the references to colour in this figure legend, the reader is referred to the web version of this article.)

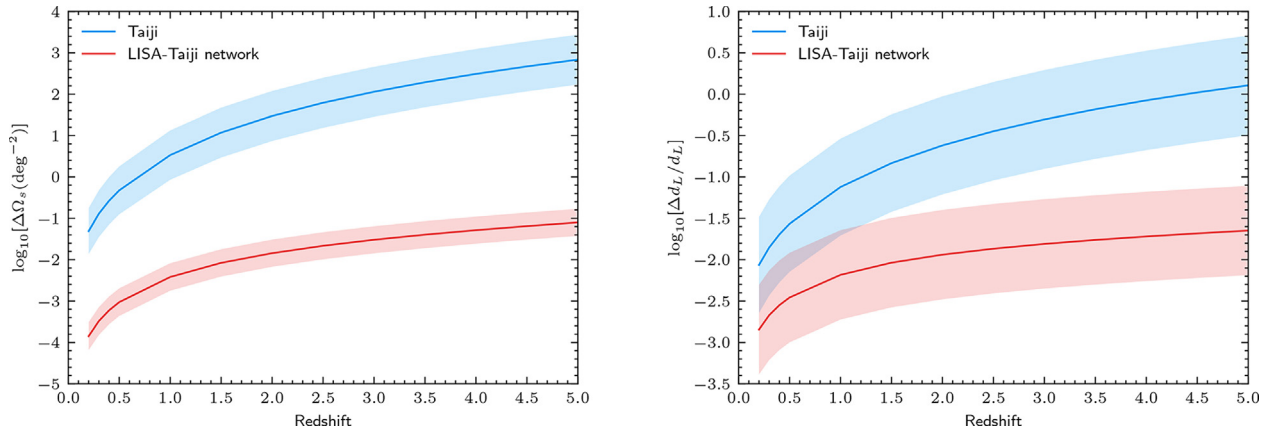


**Fig. 3.** The variation of the angular resolution  $\Delta\Omega_s$  (left panel) and the luminosity distance uncertainty  $\Delta d_L/d_L$  (right panel) with redshift for Taiji (blue) and the LISA-Taiji network (red). The shaded region corresponds to the  $1\sigma$  uncertainty range and the median value is represented by the center line. The  $1\sigma$  uncertainty range is determined based on a catalogue of 10,000 simulated equal-mass BBHs with a fixed redshift but varying sky directions and inclination angles. The total intrinsic masses of massive BBHs are fixed at  $M = 10^5 M_\odot$ . Figures from Ref [8]. (For interpretation of the references to colour in this figure legend, the reader is referred to the web version of this article.)

tational and electromagnetic observations [34]. The Fisher information matrix approach can also be used to estimate the localization accuracy of the resolved GBs. Due to the differences of the arm length and the motion of detector, LISA and Taiji has better localization accuracy and better sky coverage for the sources emitting GW signals at 1 mHz and 10 mHz, while TianQin has a better performance on the sources emitting GW signals at 100 mHz [35]. The network of the two or three detectors is capable of improving the precision of sky localization for signals within the frequency range of 1 – 100 mHz by a factor of 2 to 10 compared to a single detector, while also expanding the sky coverage for the angular resolution [23,35,36].

### 2.3. Cosmological implication in GW sirens

The better distance and sky localization determination in the network [8,27,36] will facilitate the cosmological implications, such as the GW sirens [37–39]. The GW siren method for distance measurement can be classified into two categories, namely the bright [1,40] and dark [41–43] sirens. The former relies on the EM counterpart observations to get the redshift information of the host galaxies. Due to the existence of the gas rich accretion disk, we do expect the EM counterpart flare from the massive BBH, for which can be used as the bright siren [40]. Even in the case that the flare is too faint or the jet does not point to us, we can still use the statistical method to infer the redshift of the

host galaxy, i.e., the dark siren method. There are various ways to infer the redshift, the “statistical galaxy catalog method” is one of the most faithful method [44]. The advantage of the dark siren with respect to the bright siren is that the former is much less expensive. It does not ask for the follow-up monitoring at all, but only the existence of the galaxy catalogs in the targeted sky area. The dis-advantage of the dark siren is that the redshift is completely degenerate with the distance without knowing the Hubble parameter. Hence, for single dark siren system, the distribution of the Hubble parameter posterior is multi-peaked. In order to have an accurate estimation of the Hubble parameter, we need to combine many dark siren systems. As shown in Fig. 4, the network of LISA-Taiji (wrt. Taiji-only) can significantly improve the numbers of good GW sirens, whose distance determination errors are less than 5% [37]. For GW sirens, the gravitational lensing is an unavoidable error for the distance measurement [45–47]. As shown in [37], one can see that without considering lensing noise the LISA-Taiji network could detect the events with distance error  $< 5\%$  all the way up to  $z \approx 8$ . Once, we considered this noise, the corresponding redshift reduces to  $z \sim 1.2$ . For bright sirens, the LISA-Taiji network could double the detected event numbers wrt. Taiji-only [38]. As shown by [48], in fact the counterparts detectable by LSST are always detectable by SKA + ELT. The number of LSST counterpart detections is around 1. According to the calculation in [39], within 5 years observation of massive BBH GW events by LISA, the number of the radio counterparts observed by SKA is 34; the num-

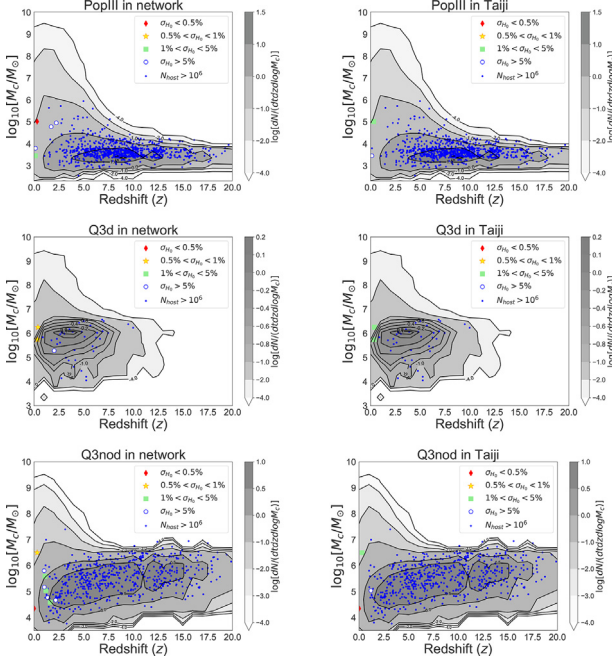


**Fig. 4.** The simulated merger event rate distribution of massive BBHs in redshift and chirp mass within 5-year observation time of the LISA-Taiji network and Taiji-only mission. Red diamonds ( $\sigma_{H_0}/H_0 < 0.5\%$ ), yellow stars ( $0.5\% - 1\%$ ), green squares ( $1\% - 5\%$ ) as well as blue circles ( $> 5\%$ ) are the classified dark sirens according to their Hubble parameter estimation accuracies. The filled blue spots are the unqualified dark sirens whose possible host galaxy numbers are more than  $10^6$  due to the poor sky localisation. The background grey contours are the theoretical massive BBH merger event rate distribution. The first column are the results in the LISA-Taiji network, while the second column are for the Taiji-only case. The first, second and third rows are the predictions from 3 different massive black hole models, namely PopIII, Q3d and Q3nod, respectively. These plots are from Ref [37]. (For interpretation of the references to colour in this figure legend, the reader is referred to the web version of this article.)

ber of the optical observations with ELT of SKA counterparts hosts is 28. For 5 years of observation of the LISA-Taiji network, the number of SKA + ELT counterparts is around 58 (if the average improvement of localization is 100 times the number is 83) [39]. Besides the Hubble parameter estimation, the network can also tell the black hole formation mechanism [49]. In particular, the joint network has the potential to observe growing light seeds in the range  $15 < z < 20$  while a single detector can hardly see, which would shed light on the light seeding mechanism.

### 3. Testing parity violation

In this section, we discuss the correlation analysis for SGWBs with space detector networks, paying special attention on the measurement of their Stokes  $V$  parameter. As in the case of electromagnetic waves, the Stokes  $V$  parameter is defined as the asymmetry between the right- and left-handed circular polarization modes and is closely related to parity violation processes.

Currently, these are many theoretical scenarios for generating chiral asymmetries ( $V \neq 0$ ) for SGWBs, including those with the Chern-Simons term (see e.g., [50–55]). With its high transparency, a SGWB could be an important fissile from the early universe, and an observational confirmation of its chiral asymmetry would have a considerable impacts on cosmological studies. Considering the observed isotropy of our universe, we set the monopole components of SGWBs as our primary target in the following.

### 3.1. Monopole pattern

We decompose the metric perturbation induced by SGWB in terms of Fourier modes as

$$h(t, \mathbf{x}) = \sum_{P=R,L} \int_{-\infty}^{\infty} df \int_{S^2} d\mathbf{n} h_P(f\mathbf{n}) \mathbf{e}^P(\mathbf{n}) e^{2\pi i f(\mathbf{n}\cdot\mathbf{x}-t)}. \quad (5)$$

Here the unit vector  $\mathbf{n}$  represents the wave propagation direction and the two tensors  $\mathbf{e}^{R,L}(\mathbf{n})$  show the right- and left-handed circular polarization bases. They are given by the linear polarization bases  $\mathbf{e}^{+,\times}$  (the plus and cross modes) as

$$\mathbf{e}^R = \frac{(\mathbf{e}^+ + i\mathbf{e}^\times)}{\sqrt{2}}, \quad \mathbf{e}^L = \frac{(\mathbf{e}^+ - i\mathbf{e}^\times)}{\sqrt{2}}. \quad (6)$$

As mentioned earlier, our main target here is the isotopic components of the background. We have two relevant modes, corresponding to the Stokes  $I$  and  $V$  parameters. They are related to the mode spectra as

$$\begin{pmatrix} \langle h_R(f\mathbf{n})h_R(f'\mathbf{n}')^* \rangle + \langle h_L(f\mathbf{n})h_L(f'\mathbf{n}')^* \rangle \\ \langle h_R(f\mathbf{n})h_R(f'\mathbf{n}')^* \rangle - \langle h_L(f\mathbf{n})h_L(f'\mathbf{n}')^* \rangle \end{pmatrix} = \frac{\delta_{\mathbf{n},\mathbf{n}'}}{4\pi} \delta_{f,f'} \begin{pmatrix} I(f) \\ V(f) \end{pmatrix} \quad (7)$$

with the Delta functions [56]. In Eq. 7, the parameter  $I$  is given as the sum of the right- and left-handed waves, representing the total intensity. On the other hand, the parameter  $V$  characterizes their asymmetry. The other two Stokes parameters  $Q$  and  $U$  do not have monopole modes, as they are related to linear polarization (introducing specific spatial direction). Using the normalized energy density  $\Omega_{\text{GW}}(f)$  and the prioritization degree  $\Pi(f)$ , we can put

$$I(f) = \frac{\rho_c}{4\pi^2 f^3} \Omega_{\text{GW}}(f), \quad V(f) = \frac{\rho_c}{4\pi^2 f^3} \Omega_{\text{GW}}(f) \Pi(f) \quad (8)$$

with the critical density of the universe  $\rho_c$ .

### 3.2. Correlation analysis

Next, let us consider a detector  $a$  (at the position  $\mathbf{x}_a$  with the detector tensor  $\mathbf{d}_a$ ) under the low frequency approximation. In the Fourier space, its reaction to the SGWB can be expressed as

$$h_a(f) = \sum_{P=R,L} \int d\mathbf{n} h_P(f\mathbf{n}) (\mathbf{d}_a : \mathbf{e}^P) e^{2\pi i f \mathbf{n} \cdot \mathbf{x}_a} \quad (9)$$

with the colon  $:$  for the double contraction of the two involved tensors. Then we consider another noise independent interferometer  $b$  and take a correlation product  $\langle h_a(f)h_b(f')^* \rangle = C_{ab}(f)\delta_{f,f'}$ . Using Eqs. 6,7 we have

$$C_{ab}(f) = \frac{8\pi}{5} [\gamma_{Iab}(f)I(f) + \gamma_{Vab}(f)V(f)]. \quad (10)$$

Here  $\gamma_{Iab}$  and  $\gamma_{Vab}$  are called the overlap reduction functions, respectively showing the sensitivity to the  $I$  and  $V$  modes. After some algebra, we have

$$\begin{aligned} \gamma_{Iab}(f) &= \frac{5}{8\pi} \int d\mathbf{n} (F_a^+ F_b^+ + F_a^\times F_b^\times) e^{2\pi i f \mathbf{n} \cdot (\mathbf{x}_a - \mathbf{x}_b)}, \\ \gamma_{Vab}(f) &= \frac{-5i}{8\pi} \int d\mathbf{n} (F_a^+ F_b^\times - F_a^\times F_b^+) e^{2\pi i f \mathbf{n} \cdot (\mathbf{x}_a - \mathbf{x}_b)} \end{aligned} \quad (11)$$

with the standard beam patten functions ( $F_a^{+,\times}(\mathbf{n}) \equiv \mathbf{d}_a : \mathbf{e}^{+,\times}(\mathbf{n})$ ) as [56–58]. We discuss the these overlap reduction functions for the LISA-Taiji and LISA-TianQin networks in the following two subsections.

### 3.3. LISA-Taiji Network

The LISA-Taiji network has an interesting geometrical symmetry [59]. In addition, a triangular detector like LISA has an internal symmetry at composing orthogonal data sets. By suitably combining these two symmetries, we can use the LISA-Taiji network as an attractive tool to explore the parity properties of a SGWB (see also [60–62]).

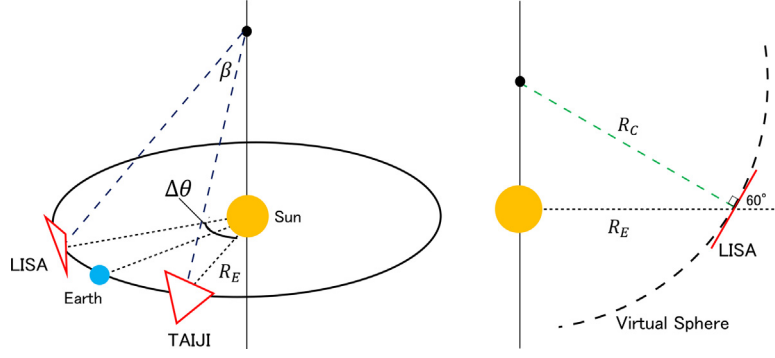


**Fig. 5. The global geometry of the LISA-Taiji network.** The two detector planes are tangential to a fixed virtual sphere of radius  $R_C = 2R_E/\sqrt{3}$  ( $R_E = 1$  a.u.: the Sun-Earth distance). The orbital phase angle is  $\Delta\theta = 40^\circ$ , corresponding to the opening angle  $\beta = 34.46^\circ$  measured from the center of the virtual sphere.

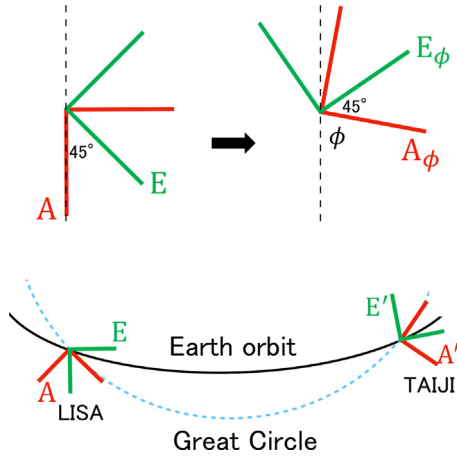


**Fig. 6. (Top) Orientation of the two effective L-shaped interferometers  $A$  and  $E$  on the detector plane.** By taking their linear combination Eq. 12, we can virtually rotate them with the new data channels ( $A_\phi, E_\phi$ ). (Bottom) By using the freedom of the rotational angle  $\phi$ , we can align the interferometer  $A$  with respect to the great circle on the virtual sphere.

As shown in Fig. 5, the detector plane of LISA is tangential to a virtual sphere of radius  $R_C = 2/\sqrt{3}R_E = 1.15$  a.u. ( $R_E = 1$  a.u.: the Sun-Earth distance). We have two options for the orientation of Taiji's detector plane. If we take the standard choice, Taiji is also tangential to LISA's virtual sphere (see Fig. 5 and also [63,64]). From the center of the sphere, the two detectors are separated by the angle  $\beta = 2\sin^{-1}[\sqrt{3}\sin(\Delta\theta/2)/2]) = 34.5^\circ$  for the orbital phase difference  $\Delta\theta = 40^\circ$ . Since a sphere is highly symmetric, it will greatly help us to figure out the underlying geometrical structure of the network.

Here we mention the additional symmetry of the system. From a LISA-like triangular detector unit, we can compose three noise orthogonal data  $A, E$  and  $T$  [65]. The  $T$  mode is much less sensitive in the frequency regime relevant for our study. Due to a systematic cancellation, we cannot probe the monopole components of a SGWB by correlating these modes. As shown in Fig. 6, in the low frequency regime, the  $A$  and  $E$  modes correspond to a pair of two L-shaped interferometer with the offset angle  $45^\circ$ , composing a symmetric base system. Importantly, by taking their linear combinations,

$$A_\phi = A \cos 2\phi + E \sin 2\phi, \quad E_\phi = -A \sin 2\phi + E \cos 2\phi, \quad (12)$$

we can effectively rotate the two interferometers by the angle  $\phi$  (see Fig. 6).

Now we couple this internal symmetry with the virtual sphere of the LISA-Taiji network. We can align the orientation of the effective L-shaped interferometers by using the great circle (geodesic) that connects LISA and Taiji on the sphere (see Fig. 6). We put the resultant effective

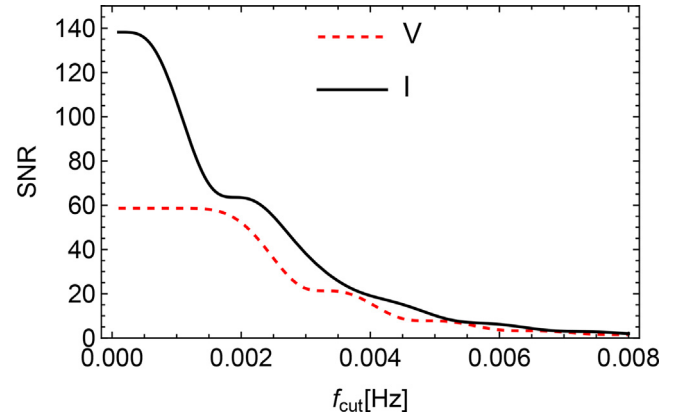


**Fig. 7. Signal-to-noise ratios for the  $I$  and  $V$  modes with  $f_{\max} = 10$  mHz and  $T_{\text{obs}} = 10$  yr.** We set  $\Omega_{\text{GW}}(f) = 10^{-11}$  and  $\Pi(f)\Omega_{\text{GW}}(f) = 10^{-11}$  for the background spectra.

interferometers simply by  $A$  and  $E$  for LISA, and  $A'$  and  $E'$  for Taiji. Then, because of the mirror symmetry of the pairwise interferometers with respect to the plane containing the great circle (and the center of the sphere), we can readily find that the combinations  $AA'$  and  $EE'$  are sensitive only to the parity even components (i.e.  $\gamma_{VAA'} = \gamma_{VEE'} = 0$ ). We similarly find  $\gamma_{IAE'} = \gamma_{IAE'} = 0$  and  $\gamma_{VEA'} = \gamma_{VEA'}$ . Furthermore, we can directly use the analytical expressions for the overlap reduction functions derived originally for the ground based detectors [10,57,58]. For example, we have

$$\gamma_{VEA'}(f) = \gamma_{VAE'}(f) = \sin \frac{\beta}{2} \left[ \left( -j_1 + \frac{7}{8}j_3 \right) + \left( j_1 + \frac{3}{8}j_3 \right) \cos \beta \right] \quad (13)$$

with the spherical Bessel function  $j_l(y)$  and its argument  $y = \pi f c^{-1} R_C \sin(\Delta\theta/2)$ .

We can now evaluate the signal-to-noise ratios  $SNR_{I,V}$  with the LISA-Taiji network, using standard expressions for the correlation analysis

$$SNR_I^2 = \left( \frac{16\pi}{5} \right)^2 T_{\text{obs}} \left[ 2 \int_{f_{\min}}^{f_{\max}} df \frac{(\gamma_{IAA}^2 + \gamma_{IEE}^2) I(f)^2}{f^6 S_L(f) S_T(f)} \right], \quad (14)$$

$$SNR_V^2 = \left( \frac{16\pi}{5} \right)^2 T_{\text{obs}} \left[ 2 \int_{f_{\min}}^{f_{\max}} df \frac{2\gamma_{VAE}^2 V(f)^2}{f^6 S_L(f) S_T(f)} \right]. \quad (15)$$

Here  $S_L(f)$  and  $S_T(f)$  represent the noise spectra of LISA and Taiji, and we are assumed to use the frequency regime  $[f_{\min}, f_{\max}]$ . In Fig. 7, we show our numerical results for flat spectral models  $\Omega_{\text{GW}} = 10^{-11}$  and  $\Pi\Omega_{\text{GW}} = 10^{-11}$ . The step-like patterns are mainly caused by the frequency dependence of the overlap reduction functions, indicating

that the importance of the contribution around 2–3 mHz. If we require the minimum signal-to-noise ratio 10, the detection threshold is  $\Omega_{\text{GW}} \sim 7 \times 10^{-13}$  and  $\Omega_{\text{GW}}\Pi \sim 1.6 \times 10^{-12}$  for a ten year correlation analysis.

### 3.4. LISA-TianQin network

Unlike the LISA-Taiji network (with the overlapped contact sphere), the LISA-TianQin network [63,66] does not have a global geometrical symmetry. While we can still use the internal symmetry of a triangle detector to simplify some of analytical expressions [63], the parity decomposition with the great circle alignment is now inapplicable. However, since the relative configuration of LISA and TianQin changes with time, we can effectively obtain the correlation products for many network geometry. By taking their appropriate linear combinations, we can algebraically separate the two parity components  $I$  and  $V$ .

If we want to decompose not only the two tensor components but also relevant vector and scalar components [61,67], this network might be advantageous, in comparison of the number of the independent correlation products and that of the target polarization components.

## 4. Subtraction of the galactic foreground

According to current models and observations, our Milky Way hosts a large number of ultracompact binaries that emit GWs in the millihertz frequency range [68–71]. The GWs from more than 20 million GBs will enter the space-based GW observation band simultaneously [72–75]. Those binaries are in the inspiral phase, millions of years before merger [70,76]. It means that the continuously emitted GWs will overlap, resulting in a foreground signal for space-based detections [68,69,77–85]. Only a few tens of thousands of them are bright enough for data analysis to be subtracted with LISA/Taiji [74,81,82,84–92]. The rest are unresolvable, forming an effective noise, known as ‘foreground confusion’ or ‘confusion noise’ [82]. The foreground confusion provides the dominant part of the noise in the frequency range of 0.5 mHz to 3 mHz [81,82,85], which will affect the detection of other GW sources [93]. Studying the evolution and distribution of GBs within our Milky Way using foreground GW signals is one of the primary scientific objectives of LISA/Taiji [6,73,76,80,94–97]. Known from electromagnetic observations, about 40 verification binaries are expected to enter the mHz band, which can be used to evaluate the performance of the mission [74,98–103]. The GW detection in a network will aid in the subtraction of GB signals and suppression of foreground confusion [104].

Many studies have been conducted on the foreground GW signals from GBs in the mHz band since LISA was proposed [69–73,77–81,83,84,95,105]. In Ref [81], the authors investigated the GB signals with the new LISA design updated in 2016. The catalog of the GBs they used contains about 26 million sources in our Milky Way [106]. The iterative procedure proposed in Ref [79], was employed to subtract the bright sources and estimate the residual confusion noise for various observation times, including  $T_{\text{obs}} = 6$  months, 1 year, 2 years, and 4 years. Approximately 29,000 thousand GBs are marked as ‘resolvable’, whose signal-to-noise ratio  $> 7$  for a 4-year observation. The analytic fit for the residual confusion noise was obtained, see Eq. (3) in Ref [81]. Most GBs are resolvable at the frequency of 2 to 3 mHz. During the procedure, it is assumed that the resolvable sources can be subtracted without any residuals. However, in real-world data analysis, inaccurate removal of these sources can introduce errors in parameter estimation [93].

In Ref [82], the updated GB catalog, which includes approximately 29.8 million sources [75], was utilized to develop the methodology for estimating the confusion noise. The authors used a new analytical form to fit the foreground confusion at signal-to-noise ratio thresholds of 5 and 7 for observation time  $T_{\text{obs}} = 0.5, 1, 2, 4,$  and 6 years:

$$S_c(f) = \frac{A}{2} f^{-7/3} e^{-(f/f_1)^\alpha} \left(1 + \tanh\left(\frac{f_{\text{knee}} - f}{f_2}\right)\right). \quad (16)$$

The fitting parameters  $A, \alpha, f_1, f_{\text{knee}},$  and  $f_2$  can be found in Table II in Ref [82]. They found that different methods for smoothing the power

spectral density yielded different results. Under a 4-year observation and with a signal-to-noise ratio threshold of 7, the number of resolvable sources with LISA is either 22,951 or 25,025, depending on the smoothing method utilized.

The authors of Ref [84], revisit this problem by employing an observationally driven population of GBs that differs from the previous population based on binary population synthesis. The observationally driven population yields about 26 million GB sources in LISA band with 60,000 of them being resolvable and a significantly different shape of the foreground confusion. The number of resolvable sources is 2–5 times that of the binary population synthesis model.

In Ref [107], the iterative procedure has been expanded to account for the effect of the detector orbiting the Sun, which causes the foreground confusion noise to vary throughout the year.

The mission design of Taiji is similar to that of LISA, but with slightly better sensitivity, allowing Taiji to extract foreground signals more effectively [6,11]. In Ref [85], the same catalog of 29.8 million GBs [75] used in Ref [82], was used to study foreground signals and confusion noise for Taiji. The foreground confusion for Taiji is estimated and fitted in the logarithmic scale by a polynomial function with observation times of 6 months, 1 year, 2 years, and 4 years:

$$S_c(f) = \exp\left(\sum_{i=0}^5 a_i \left(\log\left(\frac{f}{\text{mHz}}\right)\right)^i\right) \text{Hz}^{-1}. \quad (17)$$

The fitting parameters  $a_i$  can be found in Table I in Ref [85]. Taking into account foreground confusion noise, Taiji’s full sensitivity curve is slightly lower than LISA’s at frequencies below 0.8 mHz and around 2 mHz. With Taiji for a 4-year observation time, 29,633 sources are resolvable (signal-to-noise ratio  $> 7$ ). All the GBs that are resolvable with LISA can also be resolved with Taiji. Additionally, Taiji can subtract  $\sim 20\%$  more GB sources that have a distribution in the Milky Way consistent with that of the resolvable sources with LISA.

The ideal subtraction assumption above yields a theoretical, optimistic estimate. The actual subtraction capability of the detection depends on the data analysis methods that are implemented. To remove foreground signals in space-based detections, a number of data processing methods have been proposed. Most of the algorithms are based on Markov Chain Monte Carlo [89,91,108–111], some are based on swarm-based algorithm [92,112–114], and others utilize Gaussian process regression and genetic algorithm [115–117], etc.

Subtraction of the galactic foreground will also benefit from network observations. The authors of Ref [104], investigated resolving GB signals with the network of LISA and Taiji-mod. The ‘Taiji-mod’ is a simplified concept of Taiji, in which they put another LISA in the place of Taiji to simulate the real Taiji. So, the arm length and noise model of Taiji-mod are the same as LISA’s. The iterative subtraction method they used is based on the particle swarm optimization algorithm. For their GBSIEVER algorithm [113], they compared the network with the individual detection. They found that the LISA-Taiji-mod network can subtract  $\sim 75\%$  more sources than a single LISA. Network observation allows for reducing residual confusion noise to a level below what is achievable with a single detector. This implies that network detection has a promising future in galactic foreground subtraction. Besides, the Fisher matrix analysis for parameter estimation may be insufficient in the multi-source GB resolution problem for the extrinsic parameters.

The space-based detectors will have the potential to detect circumbinary exoplanets orbiting double white dwarfs. This topic is discussed in Refs [118–121], for LISA and Ref [122], for LISA and Taiji.

Ref [123], recently reported that stellar-mass black hole binaries could be detected using space-based detectors and their network. The results indicate that the LISA-Taiji network can detect approximately 10 such binaries, thereby demonstrating the potential for multiband gravitational wave observations in the future.

## 5. Improvement on the number of detectable BBHs

The merging processes of stellar BBHs include the inspiralling stage at early time with GW radiation in the low-frequency band ( $\sim 10^{-4}$  – 1 Hz) and the final merger with GW radiation in the high-frequency band ( $\sim 10$  – 1000 Hz). The ground-based GW observatories LIGO/Virgo have detected about 90 mergers of stellar BBHs. A number of such BBHs, inspiralling in the low-frequency band before their final merger, are expected to be detected by space borne GW detectors, such as LISA, Taiji, and TianQin, which will enable multiband observations of GWs [124–126]. The low-frequency observations provide important information in advance on when and where a BBH merger will occur for high-frequency GW observations and multiwavelength electromagnetic observations. The multi-band GW observations of stellar BBHs are also helpful for understanding the formation mechanism of stellar BBHs and their cosmic evolution, and precise test of gravity theory, etc. To realize the potential of multi-band GW observations in practice, it is crucial to have a sufficient number of stellar BBHs being detected by the space borne low-frequency GW detectors, such as LISA, Taiji, TianQin, as well as the network composed of these detectors. Below we mainly consider LISA, Taiji, and the LISA-Taiji network for demonstration purpose.

To estimate how many stellar BBHs can be detected by the low-frequency GW detectors, we generate mock stellar BBH samples according to the cosmic evolution of the BBH merger rate similar as that in [126,127]. We adopt the merger rate density of stellar BBHs given by the current LIGO/Virgo observations, i.e.,  $\frac{d^2N}{dVdt}(z=0)(1+z)^\kappa$  with the local merger rate density of  $\frac{d^2N}{dVdt}(z=0) = 19.1^{+8.6}_{-8.5} \text{ Gpc}^{-3} \text{ yr}^{-1}$  and redshift evolution slope of  $\kappa = 2.7$  [128]. We adopt the fiducial power law plus peak model for primary mass and mass ratio distribution given in [129] (see the Power Law + Peak (PP) model therein). We generate 100 realizations for stellar BBHs and then estimate the SNR for each mock stellar BBH in each realization by the observations of LISA, Taiji, or the LISA-Taiji network over a period of either 4 or 10 years. We define a stellar BBH as a “detectable” one if its SNR  $\geq 8$  regarding to either LISA, Taiji, or LISA-Taiji. For different realizations, the expected number of “detectable” stellar BBHs are different. We rank the 100 realizations according to the expected number of “detectable” stellar BBHs from small to large, and take that with 50th rank as the representative one.

Assuming a fixed observation period of 4 years, we find that LISA, Taiji, or LISA-Taiji may detect 3 – 15, 5 – 24, or 15 – 58 stellar BBHs with consideration of the uncertainty in the local merger rate density constrained by LIGO/Virgo observations. If adopting  $\frac{d^2N}{dVdt}(z=0) = 19.1 \text{ Gpc}^{-3} \text{ yr}^{-1}$ , then the expected number of “detectable” stellar BBHs is 6, 14, and 32 for LISA, Taiji, and LISA-Taiji, respectively, according to the 50th realization generated for this model. We show the distributions of the observed initial frequency and redshifted chirp mass for those “detectable” stellar BBHs in Fig. 8. As seen from this figure, none of the 6 stellar BBHs detected by LISA can merger within 4 years and only 1 can merger within 20 years; 3 of the 14 BBHs detected by Taiji can evolve to high-frequency band and merger within 4 years, and 8 of them can merger within 20 years; 3 or 17 among the 32 stellar BBHs detected by LISA-Taiji can merger within 4 or 10 years; 9 stellar BBHs have coalescence time longer than 100 years. The number of “detectable” stellar BBHs increases by a factor of  $\sim 2 - 5$  comparing with those expected by Taiji or LISA individually.

If extending the observation time to 10 years, then the expected number of “detectable” stellar BBHs increases to 33, 56, or 132 for LISA, Taiji, or LISA-Taiji according to the 50th realization from the model with  $\frac{d^2N}{dVdt}(z=0) = 19.1 \text{ Gpc}^{-3} \text{ yr}^{-1}$ . We show the observed initial frequency and redshifted chirp mass of the “detectable” mock stellar BBHs for this case in Fig. 9. As seen from this figure, LISA can detect many more stellar BBHs than the case shown in Fig. 8 but again none of them can merge within 10 years; Taiji can detect about 8 stellar BBHs that can merge within 10 years; while LISA-Taiji can detect 24 stellar BBHs that can merge within 10 years. Apparently, the network by combining LISA

and Taiji may improve substantially the detection rate of stellar BBHs in the low-frequency band and enable the multi-band studies of a substantial number of stellar BBHs, which greatly enhances the potential of multi-band observations.

We calculate the parameter estimation accuracies for those “detectable” stellar BBHs by LISA, Taiji, and LISA-Taiji, via the Fisher Information Matrix method. Figs. 10,11 show the sky localization areas and the relative errors of luminosity distance measurements for those stellar BBHs detected by LISA, Taiji, and LISA-Taiji, via the observations with a period of 4 and 10 years, respectively. Assuming an observation period of 4 years (see Fig. 10), LISA or Taiji may localize the “detectable” BBHs in sky areas ranging from  $\sim 8.1$  to  $190 \text{ deg}^2$  or  $\sim 0.33$  to  $200 \text{ deg}^2$ . LT may localize the “detectable” BBHs in sky areas in the range of  $0.22 - 190 \text{ deg}^2$ . For the common sources detected also by either LISA or Taiji, the localizations by LISA-Taiji are a factor of  $\sim 3$  or  $\sim 2$  better than those obtained by using LISA or Taiji data only. The relative errors of luminosity distances detected by LISA or Taiji both ranges from  $\sim 0.05$  to  $0.1$ . LISA-Taiji measure the luminosity distances with relative errors in the range of  $0.04 - 0.09$ . For those common sources detected also by either LISA or Taiji, LISA-Taiji gives the luminosity distance measurements slightly better than those obtained by using LISA or Taiji data only and the improvement factor is  $\sim 1.3$ . Similarly, LISA-Taiji may also help improving the measurement accuracy for  $\mathcal{M}_c$  and  $\eta$  as well. LISA or Taiji could measure  $\mathcal{M}_c$  with relative errors in the range of  $2.4 \times 10^{-5} - 1.5 \times 10^{-4}$  or  $8.6 \times 10^{-7} - 2.2 \times 10^{-4}$  and  $\eta$  with relative errors in the range of  $0.24 - 1.6$  or  $0.0061 - 2.2$ . LISA-Taiji may measure the redshifted chirp mass with relative errors in the range of  $7.1 \times 10^{-7} - 3.0 \times 10^{-4}$  and symmetric mass ratio with relative errors in the range of  $0.005 - 2.8$ . If alternatively assuming an observation period of 10 years (Fig. 11), LISA, Taiji and LISA-Taiji may localize the detectable BBHs in sky areas in the range of  $0.52 - 210 \text{ deg}^2$ ,  $0.12 - 260 \text{ deg}^2$ , and  $0.07 - 240 \text{ deg}^2$ , respectively; LISA, Taiji, and LISA-Taiji may measure the luminosity distances with relative errors in the range of  $0.032 - 0.10$ ,  $0.026 - 0.10$ , or  $0.028 - 0.12$ , measure the redshifted chirp masses with relative errors in the range of  $1.5 \times 10^{-6} - 1.1 \times 10^{-4}$ ,  $3.7 \times 10^{-7} - 1.0 \times 10^{-4}$ , or  $1.7 \times 10^{-7} - 1.5 \times 10^{-4}$ , and measure the symmetric mass ratios with relative errors in the range of  $0.011 - 1.3$ ,  $0.0027 - 1.2$ , or  $0.0016 - 2.0$ . The reason for the slight improvements by the network in localization and parameter estimations is mainly due to the enhancement of the SNRs for those sources.

In conclusion, the joint observations of LISA and Taiji may detect about several tens to a hundred stellar BBHs within an observation period of 4 – 10 years, a factor of 2 – 3 times of those obtained by using the observations by LISA or Taiji only in the same period, mainly due to the SNR enhancement and consequently the enlargement of the horizon for detection. Among these BBHs detected by LISA-Taiji, a few to twenty BBHs can merger within the observation period, which enables the multi-band GW observations and may realize the potential of multi-band GW observations in pre-warning of the high-frequency GW and the electromagnetic observations, understanding the formation mechanism of stellar BBHs, testing the gravity theory, etc. Combining the observations of LISA and Taiji may also improve the localization and measurement accuracy of the system parameters, though the improvement is not as much as that for massive binary black holes.

## 6. Alternative networks

Beyond the fiducial LISA-Taiji and LISA-TianQin networks discussed in the previous sections, alternative networks could also be formed by planned detectors, especially for the LISA-Taiji network. The TianQin mission will deploy three spacecraft in a geocentric orbit with a semi-major axis of  $\sim 10^5 \text{ km}$ , and the constellation will face to a binary white dwarf, J0806.3+1527, as a reference source [13]. Therefore, the fiducial case should be solo option for the LISA-TianQin or Taiji-TianQin network. The LISA/Taiji missions will employ an Earth-like heliocentric orbit, and its constellation will be located at  $\sim 20^\circ$  ( $\sim 5.2 \times 10^7 \text{ km}$ )



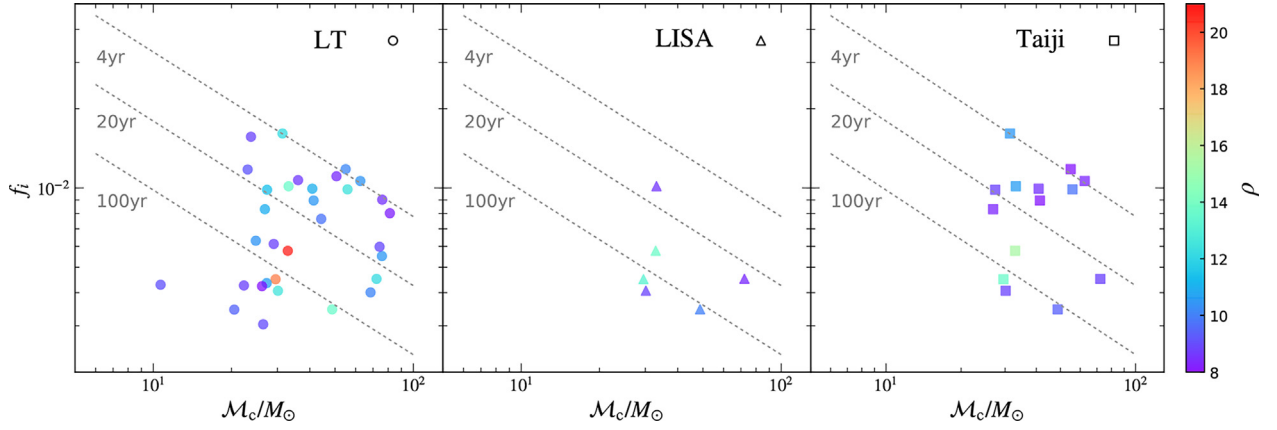


**Fig. 8.** The initial observed frequencies and redshifted chirp masses of mock stellar BBHs resulting from a realization that can be detected by the LISA-Taiji (LT) network, LISA, and Taiji, respectively. Left, middle, and right panels show those mock stellar BBHs being detected by the LISA-Taiji network with SNR  $\rho_{LT} \geq 8$ , by LISA with  $\rho_L \geq 8$ , and by Taiji with  $\rho_T \geq 8$ , respectively, over an observation period of 4 years. The color of each symbol marks the SNR of the source as indicated by the side colorbar. (For interpretation of the references to colour in this figure legend, the reader is referred to the web version of this article.)

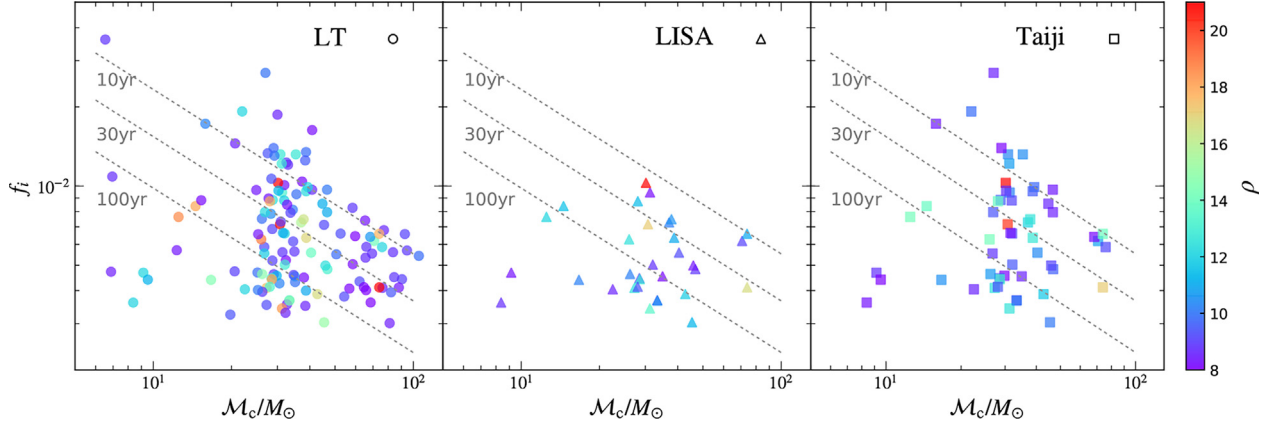


**Fig. 9.** Legend is the same as that for Fig. 8, except for an observation period of 10 years.

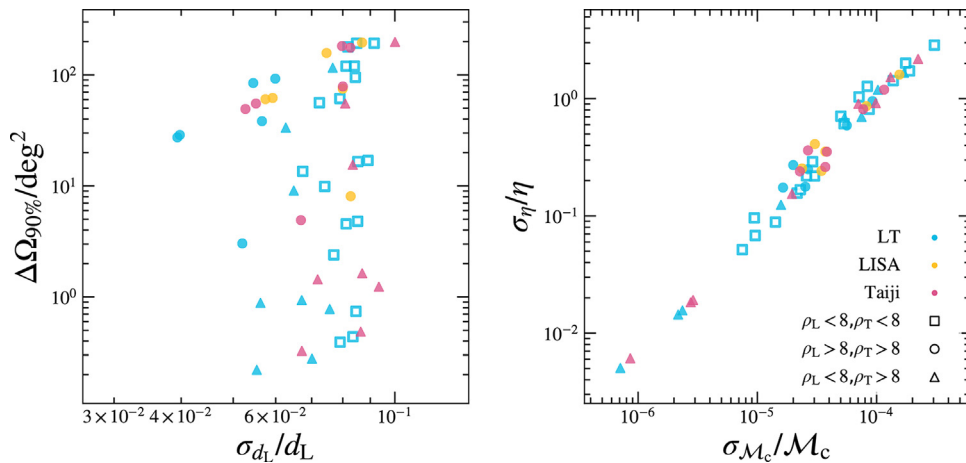


**Fig. 10.** Estimates for the errors of parameter measurements for mock stellar BBHs resulting from a realization detected by LISA, Taiji, and the LISA-Taiji (LT) network, respectively (shown in Fig. 8). Left panel shows the sky localization errors (90% confidence level) and the relative errors of luminosity distance measurements for these BBHs. Right panel shows the estimated relative errors for the redshifted chirp masses and symmetric mass ratios. Yellow, red, and cyan symbols represent those sources detected by LISA, Taiji, and the LISA-Taiji network, respectively. Circles, triangles, and squares represent those sources detected by LISA only (totally six sources), by Taiji only but not LISA (totally eight sources), and only by the LISA-Taiji network but not LISA or Taiji (totally eighteen sources), respectively. (For interpretation of the references to colour in this figure legend, the reader is referred to the web version of this article.)

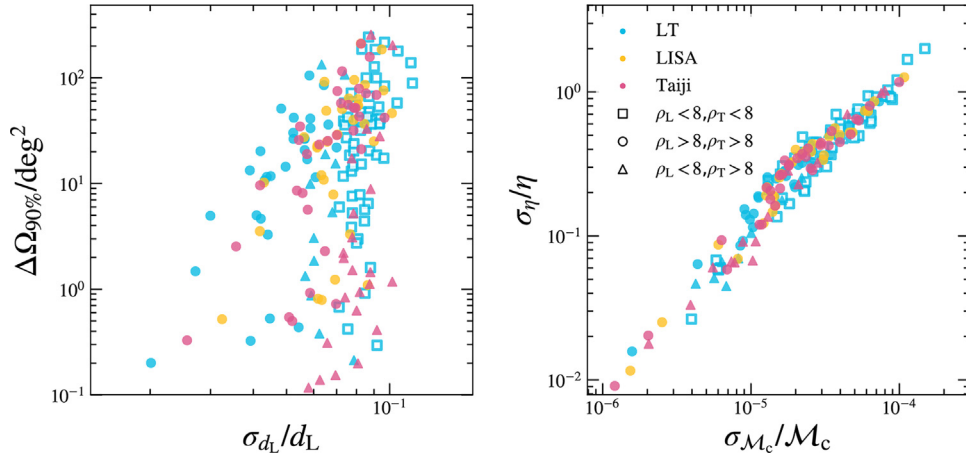


Fig. 11. Legend is the same as that for Fig. 10, except for an observation period of 10 years.

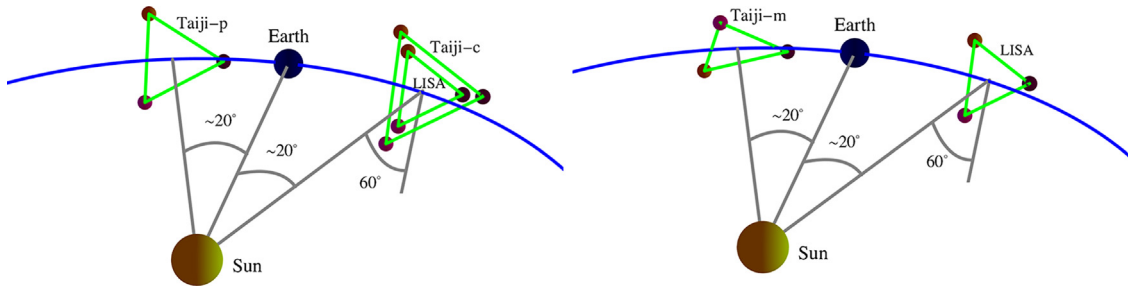


Fig. 12. Diagrams of the LISA and alternative Taiji mission orbit deployments. The left plot shows the LISA mission, which trailing the Earth by approximately 20° and is inclined by +60° with respect to the ecliptic plane. The Taiji-p leads the Earth by ~20° and is inclined by +60°. The Taiji-c is collocated and coplanar with LISA. The right panel shows the LISA and Taiji-m, which leads the Earth by ~20° and -60° inclined. The angle between the LISA and Taiji-p formation planes is ~71°, and the angle between LISA and Taiji-m formation planes is ~34.5° (recreated from [26]).

from the Earth [6,11]. This separation is a practical compromise between reducing Earth’s gravitational perturbation and the launch vehicle, telemetry capabilities [130]. The constellation plane is designed to be 60° inclined with the ecliptic plane to achieve stable interferometer arms in the Clohessy-Wiltshire framework [131].

The LISA will trail the Earth by 20°, and the formation plane is +60° inclined. Since the Taiji orbit configuration is still not fully determined, its location and orientation could be adjusted to form different networks with LISA. Three alternative LISA-Taiji networks are introduced by altering the location and orientation of the Taiji in [26,64],

- (a) Taiji-p (fiducial case), which leads the Earth by ~20° and the formation plane is +60° inclined as the LISA.
- (b) Taiji-c, which is co-located and coplanar with the LISA.
- (c) Taiji-m, which leads the Earth by ~20° and the formation plane is -60° inclined.

And the three Taiji orbital configurations are shown in Fig. 12. There also could be another Taiji orbit which trails the Earth by ~20° as LISA but with -60° orientation. And this case is ignored since it loses both the long baseline pros for the compact binary observation and full correlation with LISA for the SGWB observation. The launch budget for these three Taiji deployments should be identical/comparable, and the observation achievement should not be (statistically) different from each other. Without considering the restriction of 20° separation from the Earth, [25] examined more exhaustive Taiji orbit deployments to form the LISA-Taiji networks.

Compared to a single detector, the joint observation will promote the SNR of GW detections by a factor of  $\sim \sqrt{N_{\text{det}}}$ , where  $N_{\text{det}}$  is the number of detectors (with comparable sensitivities), and the joint SNR will be  $\rho_{\text{joint}}^2 = \sum_{i=1}^{N_{\text{det}}} \rho_i^2$ . Ref [26]. evaluated the SNRs and angular resolutions of sky localization from three LISA-Taiji networks by simulating massive BBH population with fixed masses ( $m_1 = 10^5 M_{\odot}$ ,  $m_2 = m_1/3$ ) at redshift  $z = 2$  and randomly and uniformly distributed sky directions, and the

results are shown in Fig. 13. Considering the Taiji is more sensitive than the LISA, the SNRs (in the last month before coalescences) obtained by the networks are more than  $\sim \sqrt{2}$  times higher than the single LISA as shown in the left panel. The distribution of SNRs from the joint LISA and Taiji-m observations are more concentrated compared to the other two networks, and the reason is that the Taiji-m could compensate for the LISA’s insensitive direction, and their joint response function would be more isotropic to all sky directions.

On the other hand, although the SNRs from the three networks are comparable, their capabilities of sky localization are rather different [25,26]. The first reason is that the larger separation between LISA and Taiji-p/-m could improve the resolution of sky localization, and the second reason is that the different orientations will have different antenna patterns which yield different impacts on the direction determinations. Benefiting from these two factors, as shown in the right panel of Fig. 13, the joint LISA and Taiji-m observations have the best performance on the sky localization for the sources and could improve the accuracy by a factor of ~3 orders compared to the LISA. The capability of LISA-Taiji-p is slightly worse than LISA-Taiji-m due to the suboptimal orientations, and the LISA-Taiji-c only improves the sky localization by a factor of ~2 attributed to the increase of detectors.

By employing the LISA-TianQin and alternative LISA-Taiji networks, [25] investigated the joint observations of the massive BBH from light seed (popIII) and heavy seed (Q3\_nodelay) which simulated in [132]. The capability of the LISA-Taiji-p/LISA-Taiji-m would be comparable to the LISA-TianQin to localize the BBH for the light seed scenario, and its performance become better than the LISA-TianQin for the heavy seed case because Taiji has a better sensitivity than the TianQin in the lower frequencies.

Beyond tensor polarization observations, the polarization of scalar and vector modes could also be better observed/constrained by the LISA-Taiji network. By employing the parametrized post-Einsteinian (ppE)

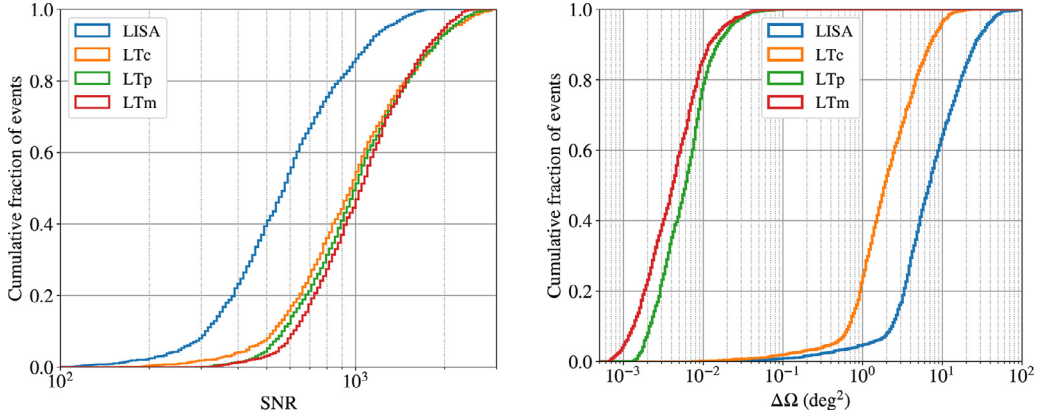


**Fig. 13.** The cumulative histograms of SNR (left panel) and angular resolution of the sky localization (right panel) from LISA and three LISA-Taiji networks (LTc: LISA with Taiji-c, LTp: LISA with Taiji-p, LTm: LISA with Taiji-m) for the massive BBH mergers (which masses  $m_1 = 10^5 M_\odot$ ,  $m_2 = m_1/3$ , at redshift  $z = 2$ , and their sky directions are random) (figures from [26]).

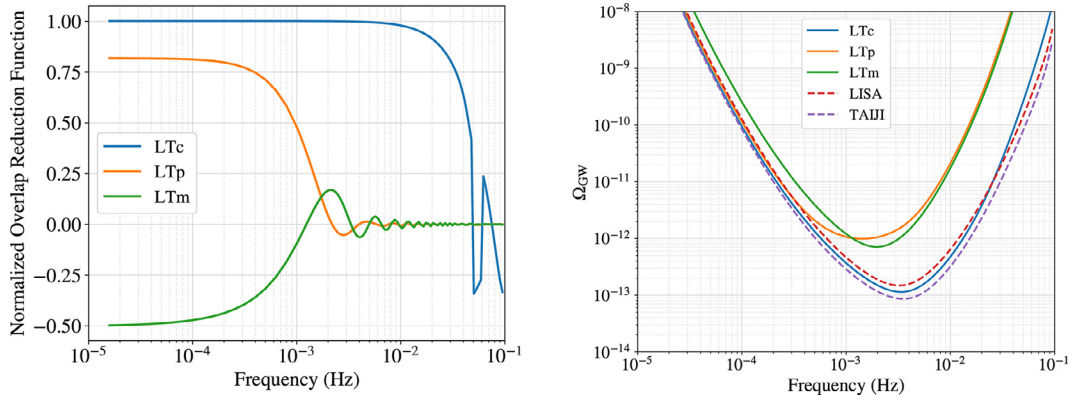


**Fig. 14.** The overlap reduction functions for tensor polarization (left) and power-law integrated sensitivities (right) of three LISA-Taiji networks (LTc: LISA with Taiji-c, LTp: LISA with Taiji-p, LTm: LISA with Taiji-m). The overlap reduction function is calculated for the tensor + and × polarizations, and the sensitivities in the right plot is obtained by assuming the SNR threshold  $\rho_{th} = 10$  in three-year observation (figures from [26,64]).

formalism developed in [133,134], the determinations of the ppE parameters are examined in [26,135]. And the results show that LISA-Taiji-m would have the best performance in three alternative networks, and it could refine the amplitudes of scalar and vector polarizations by  $\sim 10$  times compared to the single LISA.

The SGWB is another targeting GW source for space missions, it may be identified from the cross-correlation between two detectors by assuming the noises are not correlated between the two detectors. The correlation between detector  $a$  and  $b$  could be quantified by overlap reduction function (ORF) as discussed in Section 3. The normalized ORFs of three LISA-Taiji networks are shown in the left panel of Fig. 14. As we can read from the plot, the ORF of LISA-Taiji-c is unity for frequencies lower than  $\sim 10$  mHz since two detectors are coplanar at the same location. It means that SGWB observed by LISA and Taiji-c will be fully correlated, and LISA-Taiji-c will be an optimal network for the SGWB identification. Due to the separation,  $D = 1 \times 10^8$  km, between LISA and Taiji-p/-m, their ORFs quickly approach zero around a critical frequency  $f_c = c/(2D) \simeq 1.5$  mHz and oscillate and decay with the increase of frequency [136]. The amplitude of ORF from LISA-Taiji-m is lower than LISA-Taiji-p in frequencies lower than the critical frequency, and it indicates the former would have the worse capability to observe the SGWB than the latter in this band.

The power-law integrated sensitivity could be employed to illustrate the detectability of the power-law SGWB signal [137], and the sensitivities of three network configurations are shown in the right panel of Fig. 14 [64]. As we can expect, the LISA-Taiji-c is optimal for the SGWB observation. For the other two networks, the LISA-Taiji-p is more sensitive than LISA-Taiji-m for frequencies lower than  $\sim 1$  mHz, and the LISA-Taiji-m becomes more sensitive in the frequency band of  $\sim [1, 8]$  mHz

which is also the most sensitive band of the detectors. Their sensitivities converge in the higher frequency range. Based on their pros and cons at different frequencies, the performance of LISA-Taiji-p and LISA-Taiji-m could be moderately/slightly different for a specific sensible SGWB as investigated in [64].

The BBO and DECIGO are planned to place three constellations on the Earth-like heliocentric orbit and observe the GW in the deci-Hz frequency band [138,139]. The separation between two constellations will be  $\sqrt{3}$  AU, and the formation plane will be  $60^\circ$  inclined with respect to the ecliptic plane. Benefiting from the long baselines and synergetic antenna pattern, the parameters of the compact binaries could be well resolved [138].

## 7. Conclusion and prospects

The era of mHz GW detections are expected to begin in the 2030s, when multiple space-based detectors would observe various sources in the mHz frequency band simultaneously. In this work, we discuss the benefits of joint observations from space detector networks. These will offer a number of advantages, including

- More precise localization of GW sources, which will be essential for understanding their astrophysical origins.
- Improved tests of relativistic gravity, including measurements of GW polarization and the possible rotation of the cosmic polarization vector.
- Better determination of the galactic background of GWs, which will provide insights into the formation and evolution of our galaxy.
- An increase in the event rate of GW detections, including both stellar-mass black hole mergers and massive black hole mergers.

The alternative LISA-Taiji networks are examined to determine the best configuration for maximizing the scientific benefits. The Taiji-m configuration is particularly promising, and it could be a competitive configuration as the fiducial Taiji-p case. And more specific investigations should be performed before the Taiji team determines the final orbital configuration.

The joint observation of space-based GW network would significantly improve the determinations of parameters from massive BBHs. Benefiting from their large separation and complementary orientation, the parameters of sources would be measured with significant improvement compared to a single detector, especially for the sky localization. The individual detector orbits around the Sun/Earth which is equivalent to a multitude of detectors at different positions and times. This would allow for the identifications of (quasi-)periodical sources' directions. The early and quick localization from the network will be crucial for multi-messenger observation, such as those performed by the ground-based advanced LIGO and advanced Virgo observations.

The joint network would also be decisive in distinguishing SGWB from the detection noises. The SGWB encodes important information about the early Universe and binary population. It would be difficult for a single detector to separate the stochastic signals from the stochastic noise, especially for an unforeseen spectrum. With joint observations of independent detectors, similar to the SGWB search employed by the ground-based interferometers, the common signals could be extracted from the correlation between two detector's data. And the physical properties, for instance, the parity violation, could be tested with the two detectors.

A network of GW detectors operating in the same frequency band can increase the efficiency of detections. Moreover, multi-band observation, either at the same time or at different times, can also increase the number of detectable events. If the phenomenological model or theoretical template is robust, observations crossing different frequency bands would tighten the parameter estimation even more effectively. For example, with a connected binary inspiral template through mHz, deci-Hz and deca-Hz frequencies, a network of space GW detectors of LISA, Taiji, AMIGO, ET and CE will be able to enhance the parameter estimation by two orders of magnitude [127]. These enhancements will strengthen the distinguishability of various GW source models, the precision of determination of cosmological models and Hubble constant, and the co-evolution of star formation, black holes and galaxies.

In addition to the mHz missions, AU-sized arm length interferometers have been proposed to observe the GW in the sub-mHz to  $\mu$ Hz band which includes the ASTROD-GW [140,141], and references therein], Folkner's mission [142]  $\mu$ -Aries [143], and LISAMax [144]. The technologies for these missions are considered to be as ready as that for the LISA. However, their sensitivity will be limited not only by instrumental noises but also confusion foreground from binaries in our galaxy [145]. Even so, the AU-size interferometers could still be more sensitive than the Gm-sized detectors by a ratio of their arm lengths. With the low-frequency GW detector(s), the massive BBHs could be routinely observed, and their distances and redshifts would be unambiguously determined with multi-messenger observations. The cosmic evolution achieved from the observation in these frequencies will give input to the issues of dark energy and dark matter, as well as their evolution.

#### Declaration of competing interest

The authors declare that they have no conflicts of interest in this work.

#### Acknowledgments

RGC is supported in part by the National Natural Science Foundation of China (11821505). ZKG is supported in part by the National Key Research and Development Program of China (2020YFC2201501), and in part by the National Natural Science Foundation of China

(12075297 and 12235019). BH is supported in part by the National Key R&D Program of China (2021YFC2203001). CL is supported by the National Natural Science Foundation of China (12147132). YJL is partly supported by the National Key Program for Science and Technology Research and Development (2020YFC2201400, 2022YFC2205201). WTN is supported in part by the National Key R&D Program of China under (2021YFC2201901). NS is supported in part by JSPS Kakuenhi Grant-in-Aid for Scientific Research (17H06358, 19K03870 and 23K03385). GW is supported by the National Key R&D Program of China (2021YFC2201903), and National Natural Science Foundation of China (12003059).

#### References

- [1] B.F. Schutz, Determining the Hubble Constant from Gravitational Wave Observations, *Nature* 323 (1986) 310–311.
- [2] B.P. Abbott, et al., Observation of Gravitational Waves from a Binary Black Hole Merger, *Phys. Rev. Lett.* 116 (6) (2016) 061102.
- [3] B.P. Abbott, et al., GW170814: A Three-Detector Observation of Gravitational Waves from a Binary Black Hole Coalescence, *Phys. Rev. Lett.* 119 (14) (2017) 141101.
- [4] B.P. Abbott, et al., GW170817: Observation of Gravitational Waves from a Binary Neutron Star Inspiral, *Phys. Rev. Lett.* 119 (16) (2017) 161101.
- [5] C. Cutler, Angular resolution of the LISA gravitational wave detector, *Phys. Rev. D* 57 (1998) 7089–7102.
- [6] P. Amaro-Seoane, H. Audley, S. Babak, et al., Laser interferometer space antenna, arXiv preprint arXiv:1702.00786 (2017).
- [7] W.-H. Ruan, C. Liu, Z.-K. Guo, et al., The LISA-Taiji network, *Nature Astron.* 4 (2020) 108–109.
- [8] W.-H. Ruan, C. Liu, Z.-K. Guo, et al., The LISA-Taiji Network: Precision Localization of Coalescing Massive Black Hole Binaries, *Research* 2021 (2021) 6014164.
- [9] B.F. Schutz, Networks of gravitational wave detectors and three figures of merit, *Class. Quant. Grav.* 28 (2011) 125023.
- [10] N. Seto, A. Taruya, Measuring a Parity Violation Signature in the Early Universe via Ground-based Laser Interferometers, *Phys. Rev. Lett.* 99 (2007) 121101.
- [11] W.-R. Hu, Y.-L. Wu, The Taiji Program in Space for gravitational wave physics and the nature of gravity, *Natl. Sci. Rev.* 4 (5) (2017) 685–686.
- [12] W.-H. Ruan, Z.-K. Guo, R.-G. Cai, et al., Taiji program: Gravitational-wave sources, *International Journal of Modern Physics A* 35 (17) (2020) 2050075.
- [13] J. Luo, L.-S. Chen, H.-Z. Duan, et al., Tianqin: a space-borne gravitational wave detector, *Classical and Quantum Gravity* 33 (3) (2016) 035010.
- [14] Y.-M. Hu, J. Mei, J. Luo, Science prospects for space-borne gravitational-wave missions, *National Science Review* 4 (5) (2017) 683–684.
- [15] T. Bogdanović, M.C. Miller, L. Blecha, Electromagnetic counterparts to massive black-hole mergers, *Living Reviews in Relativity* 25 (1) (2022) 3.
- [16] C. Cutler, Angular resolution of the lisa gravitational wave detector, *Physical Review D* 57 (12) (1998) 7089.
- [17] T.A. Moore, R.W. Hellings, Angular resolution of space-based gravitational wave detectors, *Physical Review D* 65 (6) (2002) 062001.
- [18] N. Seto, Strong gravitational lensing and localization of merging massive black hole binaries with lisa, *Physical Review D* 69 (2) (2004) 022002.
- [19] R.N. Lang, S.A. Hughes, Measuring coalescing massive binary black holes with gravitational waves: The impact of spin-induced precession, *Physical Review D* 74 (12) (2006) 122001.
- [20] R.N. Lang, S.A. Hughes, Localizing coalescing massive black hole binaries with gravitational waves, *The Astrophysical Journal* 677 (2) (2008) 1184.
- [21] M. Trias, A.M. Sintes, Lisa observations of supermassive black holes: Parameter estimation using full post-newtonian inspiral waveforms, *Physical Review D* 77 (2) (2008) 024030.
- [22] J. Thorpe, S. McWilliams, B. Kelly, et al., Lisa parameter estimation using numerical merger waveforms, *Classical and Quantum Gravity* 26 (9) (2009) 094026.
- [23] G. Wang, W.-T. Ni, W.-B. Han, et al., Numerical simulation of sky localization for lisa-taiji joint observation, *Physical Review D* 102 (2) (2020) 024089.
- [24] C. Zhang, Y. Gong, C. Zhang, et al., Parameter estimation for space-based gravitational wave detectors with ringdown signals, *Physical Review D* 104 (8) (2021) 083038.
- [25] K.J. Shuman, N.J. Cornish, Massive black hole binaries and where to find them with dual detector networks, *Phys. Rev. D* 105 (6) (2022) 064055.
- [26] G. Wang, W.-T. Ni, W.-B. Han, et al., Alternative LISA-TAIJI networks, *Phys. Rev. D* 104 (2) (2021) 024012.
- [27] C. Zhang, Y. Gong, C. Zhang, Source localizations with the network of space-based gravitational wave detectors, *Phys. Rev. D* 106 (2) (2022) 024004.
- [28] Q. Hu, M. Li, R. Niu, et al., Joint observations of space-based gravitational-wave detectors: Source localization and implications for parity-violating gravity, *Physical Review D* 103 (6) (2021) 064057.
- [29] S. Chib, Markov chain monte carlo methods: computation and inference, *Handbook of econometrics* 5 (2001) 3569–3649.
- [30] J. Skilling, Nested sampling, in: Aip conference proceedings, volume 735, American Institute of Physics, 2004, pp. 395–405.
- [31] V. Korol, E.M. Rossi, P.J. Groot, et al., Prospects for detection of detached double white dwarf binaries with gaia, lsst and lisa, *Monthly Notices of the Royal Astronomical Society* 470 (2) (2017) 1894–1910.

- [32] A. Lamberts, S. Blunt, T.B. Littenberg, et al., Predicting the LISA white dwarf binary population in the Milky Way with cosmological simulations, *Mon. Not. Roy. Astron. Soc.* 490 (4) (2019) 5888–5903.
- [33] C. Liu, W.-H. Ruan, Z.-K. Guo, Confusion noise from galactic binaries for taiji, arXiv preprint arXiv:2301.02821 (2023).
- [34] T. Kupfer, V. Korol, S. Shah, et al., Lisa verification binaries with updated distances from gaia data release 2, *Monthly Notices of the Royal Astronomical Society* 480 (1) (2018) 302–309.
- [35] T. Jiang, Y. Gong, X. Lu, Sky localization of space-based detectors with time-delay interferometry, arXiv preprint arXiv:2301.05923 (2023).
- [36] C. Zhang, Y. Gong, H. Liu, et al., Sky localization of space-based gravitational wave detectors, *Phys. Rev. D* 103 (10) (2021) 103013.
- [37] R. Wang, W.-H. Ruan, Q. Yang, et al., Hubble parameter estimation via dark sirens with the LISA-Taiji network, *Natl. Sci. Rev.* 9 (2) (2022) nwab054.
- [38] L.-F. Wang, S.-J. Jin, J.-F. Zhang, et al., Forecast for cosmological parameter estimation with gravitational-wave standard sirens from the LISA-Taiji network, *Sci. China Phys. Mech. Astron.* 65 (1) (2022) 210411.
- [39] T. Yang, Gravitational-Wave Detector Networks: Standard Sirens on Cosmology and Modified Gravity Theory, *JCAP* 05 (2021) 044.
- [40] D.E. Holz, S.A. Hughes, Using gravitational-wave standard sirens, *Astrophys. J.* 629 (2005) 15–22.
- [41] H.-Y. Chen, M. Fishbach, D.E. Holz, A two per cent Hubble constant measurement from standard sirens within five years, *Nature* 562 (7728) (2018) 545–547.
- [42] M. Fishbach, R. Gray, I. Magaña Hernandez, et al., A Standard Siren Measurement of the Hubble Constant from GW170817 without the Electromagnetic Counterpart, *Astrophys. J. Lett.* 871 (1) (2019) L13.
- [43] R. Gray, I.M. Hernandez, H. Qi, et al., Cosmological inference using gravitational wave standard sirens: A mock data analysis, *Phys. Rev. D* 101 (12) (2020) 122001.
- [44] R. Abbott, et al., Constraints on the cosmic expansion history from GWTC-3 (2021). 2111.03604
- [45] C.M. Hirata, D.E. Holz, C. Cutler, Reducing the weak lensing noise for the gravitational wave Hubble diagram using the non-Gaussianity of the magnification distribution, *Phys. Rev. D* 81 (2010) 124046.
- [46] C. Bonvin, R. Durrer, M. Gasparini, Fluctuations of the luminosity distance, *Phys. Rev. D* 73 (2006) 023523. [Erratum: *Phys. Rev. D* 85 (2012) 029901]
- [47] C. Van Den Broeck, M. Trias, B.S. Sathyaprakash, et al., Weak lensing effects in the measurement of the dark energy equation of state with LISA, *Phys. Rev. D* 81 (2010) 124031.
- [48] N. Tamanini, C. Caprini, E. Barausse, et al., Science with the space-based interferometer eLISA. III: Probing the expansion of the Universe using gravitational wave standard sirens, *JCAP* 04 (2016) 002.
- [49] Y. Yang, W.-B. Han, Q. Yun, et al., Tracing astrophysical black hole seeds and primordial black holes with LISA-Taiji network, *Mon. Not. Roy. Astron. Soc.* 512 (4) (2022) 6217–6224.
- [50] S.H.-S. Alexander, M.E. Peskin, M.M. Sheikh-Jabbari, Leptogenesis from gravity waves in models of inflation, *Phys. Rev. Lett.* 96 (2006) 081301.
- [51] M. Satoh, S. Kanno, J. Soda, Circular Polarization of Primordial Gravitational Waves in String-inspired Inflationary Cosmology, *Phys. Rev. D* 77 (2008) 023526.
- [52] I. Obata, T. Miura, J. Soda, Chromo-Natural Inflation in the Axiverse, *Phys. Rev. D* 92 (6) (2015) 063516. [Addendum: *Phys. Rev. D* 95 (2017) 109902]
- [53] P. Adshead, M. Wyman, Chromo-Natural Inflation: Natural inflation on a steep potential with classical non-Abelian gauge fields, *Phys. Rev. Lett.* 108 (2012) 261302.
- [54] T. Kahnishvili, G. Gogoberidze, B. Ratra, Polarized cosmological gravitational waves from primordial helical turbulence, *Phys. Rev. Lett.* 95 (2005) 151301.
- [55] J. Ellis, M. Fairbairn, M. Lewicki, et al., Detecting circular polarisation in the stochastic gravitational-wave background from a first-order cosmological phase transition, *JCAP* 10 (2020) 032.
- [56] N. Seto, Prospects for direct detection of circular polarization of gravitational-wave background, *Phys. Rev. Lett.* 97 (2006) 151101.
- [57] E.E. Flanagan, The Sensitivity of the laser interferometer gravitational wave observatory (LIGO) to a stochastic background, and its dependence on the detector orientations, *Phys. Rev. D* 48 (1993) 2389–2407.
- [58] B. Allen, J.D. Romano, Detecting a stochastic background of gravitational radiation: Signal processing strategies and sensitivities, *Phys. Rev. D* 59 (1999) 102001.
- [59] N. Seto, Measuring Parity Asymmetry of Gravitational Wave Backgrounds with a Heliocentric Detector Network in the mHz Band, *Phys. Rev. Lett.* 125 (2020) 251101.
- [60] G. Orlando, M. Pieroni, A. Ricciardone, Measuring Parity Violation in the Stochastic Gravitational Wave Background with the LISA-Taiji network, *JCAP* 03 (2021) 069.
- [61] H. Omiya, N. Seto, Searching for anomalous polarization modes of the stochastic gravitational wave background with LISA and Taiji, *Phys. Rev. D* 102 (8) (2020) 084053.
- [62] G.-C. Liu, K.-W. Ng, Overlap reduction functions for a polarized stochastic gravitational-wave background in the Einstein Telescope-Cosmic Explorer and the LISA-Taiji networks (2022). 2210.16143
- [63] N. Seto, Gravitational Wave Background Search by Correlating Multiple Triangular Detectors in the mHz Band, *Phys. Rev. D* 102 (12) (2020) 123547.
- [64] G. Wang, W.-B. Han, Alternative LISA-TAIJI networks: Detectability of the isotropic stochastic gravitational wave background, *Phys. Rev. D* 104 (10) (2021) 104015.
- [65] T.A. Prince, M. Tinto, S.L. Larson, et al., The LISA optimal sensitivity, *Phys. Rev. D* 66 (2002) 122002.
- [66] Z.-C. Liang, Y.-M. Hu, Y. Jiang, et al., Science with the TianQin Observatory: Preliminary results on stochastic gravitational-wave background, *Phys. Rev. D* 105 (2) (2022) 022001.
- [67] H. Omiya, N. Seto, Correlation analysis for isotropic stochastic gravitational wave backgrounds with maximally allowed polarization degrees, *Phys. Rev. D* 104 (6) (2021) 064021.
- [68] P.L. Bender, D. Hils, Confusion noise level due to galactic and extragalactic binaries, *Class. Quant. Grav.* 14 (1997) 1439–1444.
- [69] W.A. Hiscock, S.L. Larson, J.R. Rutzahn, et al., Low frequency gravitational waves from white dwarf MACHO binaries, *Astrophys. J. Lett.* 540 (2000) L5–L8.
- [70] G. Nelemans, L.R. Yungelson, S.F. Portegies Zwart, The gravitational wave signal from the galactic disk population of binaries containing two compact objects, *Astron. Astrophys.* 375 (2001) 890–898.
- [71] A. Lamberts, S. Blunt, T.B. Littenberg, et al., Predicting the LISA white dwarf binary population in the Milky Way with cosmological simulations, *Mon. Not. Roy. Astron. Soc.* 490 (4) (2019) 5888–5903. 1907.00014
- [72] S. Yu, C.S. Jeffery, The gravitational wave signal from diverse populations of double white dwarf binaries in the Galaxy, *Astron. Astrophys.* 521 (2010) A85.
- [73] G. Nelemans, Galactic binaries with eLISA, *ASP Conf. Ser.* 467 (2013) 27–36.
- [74] V. Korol, E.M. Rossi, P.J. Groot, et al., Prospects for detection of detached double white dwarf binaries with Gaia, LSST and LISA, *Mon. Not. Roy. Astron. Soc.* 470 (2) (2017) 1894–1910.
- [75] V. Korol, et al., Populations of double white dwarfs in Milky Way satellites and their detectability with LISA, *Astron. Astrophys.* 638 (2020) A153.
- [76] T.R. Marsh, Double white dwarfs and LISA, *Class. Quant. Grav.* 28 (2011) 094019.
- [77] N. Seto, Annual modulation of the galactic binary confusion noise background and LISA data analysis, *Phys. Rev. D* 69 (2004) 123005.
- [78] L. Barack, C. Cutler, Confusion noise from LISA capture sources, *Phys. Rev. D* 70 (2004) 122002.
- [79] S.E. Timpano, L.J. Rubbo, N.J. Cornish, Characterizing the galactic gravitational wave background with LISA, *Phys. Rev. D* 73 (2006) 122001.
- [80] S. Nissanke, M. Vallisneri, G. Nelemans, et al., Gravitational-wave emission from compact Galactic binaries, *Astrophys. J.* 758 (2012) 131.
- [81] N. Cornish, T. Robson, Galactic binary science with the new LISA design, *J. Phys. Conf. Ser.* 840 (1) (2017) 012024.
- [82] N. Karnesis, S. Babak, M. Pieroni, et al., Characterization of the stochastic signal originating from compact binary populations as measured by LISA, *Phys. Rev. D* 104 (4) (2021) 043019.
- [83] G. Boileau, A. Lamberts, N.J. Cornish, et al., Spectral separation of the stochastic gravitational-wave background for LISA in the context of a modulated Galactic foreground, *Mon. Not. Roy. Astron. Soc.* 508 (1) (2021) 803–826. [Erratum: *Mon. Not. Roy. Astron. Soc.* 508 (2021) 5554–5555]
- [84] V. Korol, N. Hallakoun, S. Toonen, et al., Observationally driven Galactic double white dwarf population for LISA, *Mon. Not. Roy. Astron. Soc.* 511 (4) (2022) 5936–5947.
- [85] C. Liu, W.-H. Ruan, Z.-K. Guo, Confusion noise from Galactic binaries for Taiji, *Phys. Rev. D* 107 (6) (2023) 064021.
- [86] R. Umstätter, N. Christensen, M. Hendry, et al., LISA source confusion: Identification and characterization of signals, *Class. Quant. Grav.* 22 (2005) S901–S912.
- [87] R. Umstätter, N. Christensen, M. Hendry, et al., Bayesian modeling of source confusion in LISA data, *Phys. Rev. D* 72 (2005) 022001.
- [88] E.D.L. Wickham, A. Stroeer, A. Vecchio, A Markov chain Monte Carlo approach to the study of massive black hole binary systems with LISA, *Class. Quant. Grav.* 23 (2006) S819–S828.
- [89] J. Crowder, N. Cornish, A Solution to the Galactic Foreground Problem for LISA, *Phys. Rev. D* 75 (2007) 043008.
- [90] A. Blaut, S. Babak, A. Krolak, Mock LISA Data Challenge for the galactic white dwarf binaries, *Phys. Rev. D* 81 (2010) 063008.
- [91] T.B. Littenberg, A detection pipeline for galactic binaries in LISA data, *Phys. Rev. D* 84 (2011) 063009.
- [92] Y. Lu, E.-K. Li, Y.-M. Hu, et al., An Implementation of Galactic White Dwarf Binary Data Analysis for MLDC-3.1, *Res. Astron. Astrophys.* 23 (1) (2023) 015022.
- [93] T. Robson, N. Cornish, Impact of galactic foreground characterization on a global analysis for the LISA gravitational wave observatory, *Class. Quant. Grav.* 34 (24) (2017) 244002.
- [94] M.R. Adams, N.J. Cornish, T.B. Littenberg, Astrophysical Model Selection in Gravitational Wave Astronomy, *Phys. Rev. D* 86 (2012) 124032.
- [95] K. Breivik, C.M.F. Mingarelli, S.L. Larson, Constraining Galactic Structure with the LISA White Dwarf Foreground, *Astrophys. J.* 901 (1) (2020) 4.
- [96] Z. Luo, Z. Guo, G. Jin, et al., A brief analysis to taiji: Science and technology, *Results in Physics* 16 (2020) 102918.
- [97] M. Georgousi, N. Karnesis, V. Korol, et al., Gravitational waves from double white dwarfs as probes of the milky way, *Mon. Not. Roy. Astron. Soc.* 519 (2) (2022) 2552–2566.
- [98] A. Stroeer, A. Vecchio, The LISA verification binaries, *Class. Quant. Grav.* 23 (2006) S809–S818.
- [99] S. Shah, G. Nelemans, Constraining parameters of white-dwarf binaries using gravitational-wave and electromagnetic observations, *Astrophys. J.* 790 (2014) 161.
- [100] K.B. Burdge, et al., General relativistic orbital decay in a seven-minute-orbital-period eclipsing binary system, *Nature* 571 (7766) (2019) 528–531.
- [101] K.B. Burdge, et al., Orbital Decay in a 20 Minute Orbital Period Detached Binary with a Hydrogen Poor Low Mass White Dwarf, *Astrophys. J. Lett.* 886 (1) (2019) L12.
- [102] W.R. Brown, M. Kilic, A. Bédard, et al., A 1201 s Orbital Period Detached Binary: The First Double Helium Core White Dwarf LISA Verification Binary, *Astrophys. J. Lett.* 892 (2) (2020) L35.

- [103] T. Kupfer, et al., LISA Galactic binaries with astrometry from Gaia DR3 (2023). ArXiv:2302.12719. 2302.12719
- [104] X.-H. Zhang, S.-D. Zhao, S.D. Mohanty, et al., Resolving Galactic binaries using a network of space-borne gravitational wave detectors, *Phys. Rev. D* 106 (10) (2022) 102004.
- [105] N.J. Cornish, T.B. Littenberg, Tests of Bayesian Model Selection Techniques for Gravitational Wave Astronomy, *Phys. Rev. D* 76 (2007) 083006.
- [106] S. Toonen, G. Nelemans, S. Portegies Zwart, Supernova Type Ia progenitors from merging double white dwarfs: Using a new population synthesis model, *Astron. Astrophys.* 546 (2012) A70.
- [107] M.C. Digman, N.J. Cornish, LISA Gravitational Wave Sources in a Time-varying Galactic Stochastic Background, *Astrophys. J.* 940 (1) (2022) 10.
- [108] J. Crowder, N.J. Cornish, Extracting galactic binary signals from the first round of Mock LISA data challenges, *Class. Quant. Grav.* 24 (2007) S575–S586.
- [109] A. Stroeer, et al., Inference on white dwarf binary systems using the first round Mock LISA Data Challenges data sets, *Class. Quant. Grav.* 24 (2007) S541–S550.
- [110] T. Littenberg, N. Cornish, K. Lackeos, et al., Global Analysis of the Gravitational Wave Signal from Galactic Binaries, *Phys. Rev. D* 101 (12) (2020) 123021.
- [111] T.B. Littenberg, N.J. Cornish, Prototype global analysis of LISA data with multiple source types, *Phys. Rev. D* 107 (6) (2023) 063004.
- [112] Y. Bouffanaï, E.K. Porter, Detecting compact galactic binaries using a hybrid swarm-based algorithm, *Phys. Rev. D* 93 (6) (2016) 064020.
- [113] X. Zhang, S.D. Mohanty, X. Zou, et al., Resolving Galactic binaries in LISA data using particle swarm optimization and cross-validation, *Phys. Rev. D* 104 (2021) 024023.
- [114] P. Gao, X.-L. Fan, Z.-J. Cao, et al., Fast resolution of Galactic binaries in LISA data, *Phys. Rev. D* 107 (12) (2023) 123029.
- [115] J. Crowder, N.J. Cornish, L. Reddinger, Darwin meets Einstein: LISA data analysis using genetic algorithms, *Phys. Rev. D* 73 (2006) 063011.
- [116] S.H. Strub, L. Ferraioli, C. Schmelzbach, et al., Bayesian parameter estimation of Galactic binaries in LISA data with Gaussian process regression, *Phys. Rev. D* 106 (6) (2022) 062003.
- [117] S.H. Strub, L. Ferraioli, C. Schmelzbach, et al., Accelerating global parameter estimation of gravitational waves from Galactic binaries using a genetic algorithm and GPUs (2023). ArXiv:2307.03763. 2307.03763
- [118] N. Seto, Detecting Planets around Compact Binaries with Gravitational Wave Detectors in Space, *Astrophys. J. Lett.* 677 (2008) L55–L58.
- [119] K.W.K. Wong, E. Berti, W.E. Gabella, et al., On the possibility of detecting ultrashort period exoplanets with LISA, *Mon. Not. Roy. Astron. Soc.* 483 (1) (2019) L33–L36.
- [120] N. Tamanini, C. Danielski, The gravitational-wave detection of exoplanets orbiting white dwarf binaries using LISA, *Nature Astron.* 3 (9) (2019) 858–866.
- [121] C. Danielski, V. Korol, N. Tamanini, et al., Circumbinary exoplanets and brown dwarfs with the Laser Interferometer Space Antenna, *Astron. Astrophys.* 632 (2019) A113.
- [122] Y. Kang, C. Liu, L. Shao, Prospects for Detecting Exoplanets around Double White Dwarfs with LISA and Taiji, *Astron. J.* 162 (6) (2021) 247.
- [123] J. Chen, C.-S. Yan, Y.-J. Lu, et al., On detecting stellar binary black holes via the LISA-Taiji network, *Res. Astron. Astrophys.* 21 (11) (2021) 285.
- [124] A. Sesana, Prospects for Multiband Gravitational-Wave Astronomy after GW150914, *Phys. Rev. Lett.* 116 (23) (2016) 231102.
- [125] S. Liu, Y.-M. Hu, J.-d. Zhang, et al., Science with the TianQin observatory: Preliminary results on stellar-mass binary black holes, *Phys. Rev. D* 101 (10) (2020) 103027.
- [126] J. Chen, C. Yan, Y. Lu, et al., On Dark Gravitational Wave Standard Sirens as Cosmological Inference and Forecasting the Constraint on Hubble Constant using Binary Black Holes Detected by Deci-hertz Observatory, *Research in Astronomy and Astrophysics* 22 (1) (2022) 015020.
- [127] Y. Zhao, Y. Lu, C. Yan, et al., Multiband gravitational wave observations of stellar binary black holes at the low to middle and high frequencies, *Monthly Notices of the Royal Astronomical Society* 522 (2) (2023) 2951–2966.
- [128] The LIGO Scientific Collaboration, the Virgo Collaboration, and the KAGRA Collaboration. GWTC-3: Compact Binary Coalescences Observed by LIGO and Virgo During the Second Part of the Third Observing Run, arXiv e-prints (2021). arXiv:2111.03606
- [129] The LIGO Scientific Collaboration, the Virgo Collaboration, and the KAGRA Collaboration. The population of merging compact binaries inferred using gravitational waves through GWTC-3, arXiv e-prints (2021). arXiv:2111.03634
- [130] LISA Study Team. LISA (Laser Interferometer Space Antenna): A Cornerstone Mission for the Observation of Gravitational Waves Technical Report, ESA-SCI, 2000. System and Technology Study Report
- [131] S.V. Dhurandhar, K. Rajesh Nayak, S. Koshti, et al., Fundamentals of the LISA stable flight formation, *Class. Quant. Grav.* 22 (2005) 481–488.
- [132] A. Klein, et al., Science with the space-based interferometer eLISA: Supermassive black hole binaries, *Phys. Rev. D* 93 (2) (2016) 024003.
- [133] N. Yunes, F. Pretorius, Fundamental Theoretical Bias in Gravitational Wave Astrophysics and the Parameterized Post-Einsteinian Framework, *Phys. Rev. D* 80 (2009) 122003.
- [134] K. Chatziioannou, N. Yunes, N. Cornish, Model-Independent Test of General Relativity: An Extended post-Einsteinian Framework with Complete Polarization Content, *Phys. Rev. D* 86 (2012) 022004. [Erratum: *Phys.Rev.D* 95 (2017) 129901]
- [135] G. Wang, W.-B. Han, Observing gravitational wave polarizations with the LISA-TAIJI network, *Phys. Rev. D* 103 (6) (2021) 064021.
- [136] J.D. Romano, N.J. Cornish, Detection methods for stochastic gravitational-wave backgrounds: a unified treatment, *Living Rev. Rel.* 20 (1) (2017) 2.
- [137] E. Thrane, J.D. Romano, Sensitivity curves for searches for gravitational-wave backgrounds, *Phys. Rev. D* 88 (12) (2013) 124032.
- [138] J. Crowder, N.J. Cornish, Beyond LISA: Exploring future gravitational wave missions, *Phys. Rev. D* 72 (2005) 083005.
- [139] S. Kawamura, et al., The Japanese space gravitational wave antenna DECIGO, *Class. Quant. Grav.* 23 (2006) S125–S132.
- [140] W.-T. Ni, ASTROD-GW: Overview and Progress, *Int. J. Mod. Phys. D* 22 (2013) 1341004.
- [141] W.-T. Ni, Gravitational wave detection in space, *Int. J. Mod. Phys. D* 25 (14) (2016) 1630001.
- [142] J. Baker, et al., Space Based Gravitational Wave Astronomy Beyond LISA, *Bull. Am. Astron. Soc.* 51 (7) (2019) 243.
- [143] A. Sesana, et al., Unveiling the gravitational universe at  $\mu$ -Hz frequencies, *Exper. Astron.* 51 (3) (2021) 1333–1383.
- [144] W. Martens, M. Khan, J.-B. Bayle, LISAmx: Improving the Gravitational-Wave Sensitivity by Two Orders of Magnitude (2023). ArXiv:2304.08287. 2304.08287
- [145] G. Wang, Z. Yan, B. Hu, et al., Investigating galactic double white dwarfs for sub-mHz gravitational wave missions ASTROD-GW, *Phys. Rev. D* 107 (12) (2023) 124022.



**Bin Hu** (BRID: 06996.00.81252) is a full professor in astronomy at Beijing Normal University. He awarded the Chinese National Youth Thousand Talents fellow in 2016. His research interests include gravitational wave, lensing and cosmology.



**Youjun Lu** (BRID: 09711.00.25079) is currently a research professor at National Astronomical Observatories of China. He was graduated from Anhui university at 1992 with a Bachelor in Physics, and he obtained his Ph.D. in astrophysics from University of Science and Technology of China. His main research includes black hole physics, gravitational wave astrophysics, Active Galactic Nuclei/QSOs, galaxies and cosmology.



**Naoki Seto** is currently an assistant professor in the Department of Physics at Kyoto University. He obtained his PhD at Kyoto University. His research interests include gravitational wave astronomy and observational cosmology.



**Yue-Liang Wu** is a well-known theoretical physicist, the member of Chinese Academy of Sciences, TWAS and International Eurasian Academy of Sciences. He currently serves as the Academic Vice-President of University of Chinese Academy of Sciences, the Director of International Centre for Theoretical Physics Asia-Pacific, the Director of Academic Science Committee of Institute of Theoretical Physics, Chinese Academy of Sciences. The chief scientist of the Taiji Program in Space for Gravitational Wave Detection in China.